Optimized Configuration of Location and Size for DGs and SCs in Radial Distributed Networks Based on Improved Butterfly Algorithm

Gonggui Chen, Xinxin Zhao, Kang Peng, Ping Zhou, Xianjun Zeng, Hongyu Long* and Mi Zou

***Abstract*—The optimal configuration problem of distributed generators (DGs) and shunt capacitors (SCs) in a radial distributed network (RDN) is to find the best installation locations and optimal capacities of DGs and SCs for optimizing a certain performance indicator. The discontinuity characteristic and huge computation of optimizing DGs and SCs in RDN make it no longer applicable by traditional methods. In this paper, a new bus processing method and an improved butterfly algorithm are proposed to solve the optimal configuration of DGs and SCs. The method of processing nodes considers not only the power loss index (*PLI*) but also the voltage amplitude of the original system, forming a sequence of candidate nodes to guide algorithm to optimizing, which can simplify the algorithm search space and improve search efficiency. Meanwhile, the butterfly algorithm with constriction factor (BF-CF) combines the inertia coefficient to introduce a constriction factor, improves the speed update model and the local search pattern, and overcomes the disadvantages of the original butterfly algorithm which is easy to fall into the local optimum and the precision of result is not high. To verify the performance of the proposed method, minimizing the active power loss and voltage deviation are selected as the objective function and reactive power loss and the worst voltage are taken as reference targets, which are performed in three standard test systems of 33-bus, 69-bus and 119-bus, respectively. The simulation results illustrate that, compared with the original butterfly algorithm and other intelligent algorithms, the method proposed in this paper has more obvious advantages and performance in solving the configuration problem of DGs and SCs in systems of various scales.**

***Index Terms*—Power Loss Index (*PLI*), Distributed Generators (DGs), Shunt Capacitors (SCs), Enhanced Butterfly Algorithm.**

Manuscript received June 10, 2021; revised December 14, 2021. This work was supported by the National Natural Science Foundation of China (51207064), the Chongqing Natural Science Foundation (cstc2020jcyj-msxmX0368), the Science and Technology Research Program of Chongqing Municipal Education Commission (KJQN201900627), the Natural Science Foundation of Chongqing (cstc2020jcyj-msxmX0693), the National Natural Science Foundation of China (52007022), and the China Postdoctoral Science Foundation (2021M693930).

Gonggui Chen is a professor of Key Laboratory of Industrial Internet of Things and Networked Control, Ministry of Education, Chongqing University of Posts and Telecommunications, Chongqing 400065, China (e-mail: chenggpower@ 126.com).

Xinxin Zhao is a master degree candidate of Chongqing University of Posts and Telecommunications, Chongqing 400065, China (e-mail: zxx_cqupt@163.com).

Kang Peng is a senior engineer of Economic and Technology Research Institute, State Grid Chongqing Electric Power Company, Chongqing 401120, China (e-mail: 1060846892@qq.com).

Ping Zhou is a senior engineer of Economic and Technology Research Institute, State Grid Chongqing Electric Power Company, Chongqing 401120, China (e-mail: 153326062@qq.com).

Xianjun Zeng is a senior engineer of State Grid Chongqing Electric Power Company, Chongqing 400015, China (e-mail: 13594255525@139.com).

Hongyu Long is a professor level senior engineer of Chongqing Key Laboratory of Complex Systems and Bionic Control, Chongqing University of Posts and Telecommunications, Chongqing 400065, China (corresponding author to provide phone: +8613996108500; e-mail: longhongyu20@163.com).

Mi Zou is an assistant professor of Chongqing Key Laboratory of Complex Systems and Bionic Control, Chongqing University of Posts and Telecommunications, Chongqing 400065, China (e-mail: zoumi@cqupt.edu.cn).

I. Introduction

With the rapid development of information technology, the global demand for electricity has sharply increased, and some new energy sources (such as wind and solar energy) have been integrated into the power grid, which poses serious challenges to the power system. Therefore, some heuristic intelligent algorithms, include Multi-objective Improved Bat Algorithm (MOIBA) [1], Quasi-oppositional Cuckoo Search Algorithm (QCSA) [2] and Gravitational Search Algorithm (GA) [3] are used to optimize the power system, to meet the requirements of power supply reliability and safety. The process of network updating will be retarded using distributed power generation technology, so as to save costs. Economic concerns above and certain environmental issues (carbon emissions) make distributed generation become the research focus of power grid technology [4, 5].

It will inevitably complicate the operation and control of power systems that integrate DGs into the grid [6]. The location and capacity of DGs are selected inappropriately, which will cause certain problems such as increased power loss and over voltage. The proper configuration of DGs can improve the voltage distribution and reduce the active and reactive power losses of the grid effectively [7, 8]. Power loss is an important indicator of power transmission performance, so reducing the power loss is the main goal of configuring DGs in [7, 9, 10]. In [11, 12], efforts are made to improve the voltage profile in distributed networks. Additionally, reference [13] also proposes targets including voltage deviation, voltage stability margin, and operating cost for configuring DGs.

In recent years, various heuristic search algorithms have been utilized to optimize the location and capacity of distributed generators and shunt capacitors to enhance the operation performance of power systems. Authors in [14] propose a hybrid Analytical Tree Growth Algorithm (ATGA) for optimizing the location and size of multiple types of DGs, and the result illustrates that active power loss obtained by

ATGA is significantly reduced with fast convergence rate. In order to reduce the power loss of the system and ameliorate the voltage stability, multi-objective search method QOSIMBO-Q is applied to configure DGs [15]. Authors in [16] put a new hybrid genetic particle swarm optimization method (HGAPSO) to determine the optimal configuration of distributed generators, which has the advantages of both GA and PSO. Compared with other methods, HGAPSO not only can improve the power loss and the voltage level of the system remarkably, but also has obvious preponderance in convergence speed.

What's more, reactive power is one of the significant factors affecting the performance of power transmission systems. Configuring shunt capacitors in the network has many advantages, such as reducing real power loss, boosting voltage distribution and promoting power factor. Therefore, in recent studies, intelligent algorithms have been applied to optimize the site and size of DGs and SCs at the same time. Authors in [17] use the constriction factor particle swarm optimization (CF-PSO) algorithm to optimize the configuration of DGs and SCs, which achieves the optimization of certain single-objective of power loss, voltage distribution, voltage stability, and voltage deviation. Configuring DGs and SCs simultaneously by hybrid method based on Genetic Algorithm (GA) and Artificial Bee Colony (ABC) for minimizing real power loss is better than GA/PSO and ICA/GA in search results and convergence speed [18]. Hybrid HS-PABC [19] optimizes the location and size of distributed generators and capacitors simultaneously in IEEE-69 and IEEE-118 systems with satisfactory optimization results. Additionally, aimed at different objectives, other intelligent algorithms such as PABC [20], ICA/GA [21] and hybrid BFO [22] achieve satisfactory results in configuring DGs and SCs.

Algorithms above randomly determine certain nodes as the installation locations of DGs and SCs in the course of the optimization process, which complicates the process of calculation. It will take a long time to reach convergence for configuring DGs and SCs collectively in large systems by traditional algorithms. To optimize the search space, the candidate buses are processed considering the power loss index and the node voltage level for guiding optimization of sites in this paper. The constriction factor is introduced in the original butterfly (BF) algorithm, and an improved butterfly algorithm (BF-CF) is proposed. The results reveal that the method in this paper is superior to other algorithms in optimization results and convergence speed.

The arrangement of this paper is as follows. Relevant mathematical models, objective functions and constraints are introduced in section II. Section III includes the description and enhancement of the algorithm. In section IV, simulation results and analysis are presented followed by conclusions in section V.

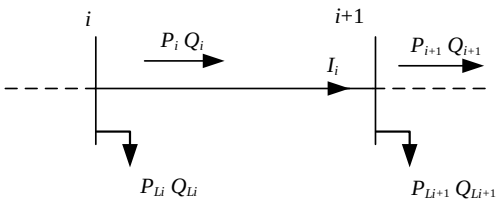

Fig. 1 Single-line structure in radial distributed network

II. Mathematical Description

The optimal configuration of DGs and SCs contains some objective functions and constraints. In this section, three objective functions of active power loss (P_T), reactive power loss (Q_T) and voltage deviation (VD) are given, then limitations of electrical parameters and size ranges of DGs and SCs are listed.

A. Objective functions

The configuration of DGs and SCs is to determine their positions and capacity under the condition of satisfying all constraints, so that the power loss and voltage deviation of the power system can be minimized. Fig. 1 shows the diagram of single-line structure in the radial network.

When the power system operates stably, the real power and reactive power from bus i and voltage of each node satisfy equations as follows [4].

$$P_i = P_{i+1} + P_{Li+1} + R_{i,i+1}\frac{P_i^2+Q_i^2}{|V_i|^2} \tag{1}$$

$$Q_i = Q_{i+1} + Q_{Li+1} + X_{i,i+1}\frac{P_i^2+Q_i^2}{|V_i|^2} \tag{2}$$

$$|V_{i+1}|^2 = |V_i|^2 - 2(R_{i,i+1}\cdot P_i + X_{i,i+1}\cdot Q_i) + (X_{i,i+1}{}^2 + R_{i,i+1}{}^2)\cdot\frac{P_i^2+Q_i^2}{|V_i|^2} \tag{3}$$

where, P_i and Q_i are the active power and reactive power flowing from bus i to bus i+1 respectively. P_{Li+1} and Q_{Li+1} are the load power at bus i+1. $R_{i,\ i+1}$ and $X_{i,\ i+1}$ represent the resistance value and inductance value between node i and node i+1, and $|V_i|$ is the voltage magnitude at node i. The last term in Eq. (1) and Eq. (2) are the real power loss and reactive power loss on branch i calculated by the following equations.

$$P_{Loss}(i,i+1) = R_{i,i+1}\cdot I_i^2 = R_{i,i+1}\cdot\frac{P_i^2+Q_i^2}{|V_i|^2} \tag{4}$$

$$Q_{Loss}(i,i+1) = X_{i,i+1}\cdot I_i^2 = X_{i,i+1}\cdot\frac{P_i^2+Q_i^2}{|V_i|^2} \tag{5}$$

where, I_i represents the current value flowing from bus i to bus i+1. The total power loss in the radial network equals the sum of power loss of all branches as follows.

$$P_T = \sum_{i=1}^{n} P_{Loss}(i,i+1) \tag{6}$$

$$Q_T = \sum_{i=1}^{n} Q_{Loss}(i,i+1) \tag{7}$$

where, n is the total number of branches in the network. P_T and Q_T represent the total active power loss and total reactive power loss of the system, respectively. In addition, the voltage deviation of the network can be calculated by Eq. (8).

$$VD = \sum_{i=1}^{N}(V_i - V_f)^2 \tag{8}$$

where, N represents the total number of buses and the voltage of reference bus is represented by V_f. Minimizing P_T and VD are the main objectives of configuring DGs and SCs in this paper. Meanwhile, Q_T is selected as a reference indicator to evaluate the overall performance of the algorithm proposed.

It will reduce the search space of the algorithm by preprocessing these candidate buses in the optimization process. The method applied in this paper is *PLI* [9]. First of

all, the active power loss of the original network is obtained by the power flow calculation. Then, by compensating for the active and reactive power of a certain node, the reductions in active and reactive power losses of each node are obtained. The power loss indices are obtained by normalizing into the range of [0,1], which can be calculated by following equation.

$$PLI = \frac{Loss\ reduction(i) - Loss\ reduction_{min}}{Loss\ reduction_{max} - Loss\ reduction_{min}} \quad (9)$$

B. Restrained Conditions

In the process of power flow calculation, the following constraints should be met.

(1) The balance of power flow should satisfy the Eq. (1) and Eq. (2). Eq. (3) for voltage must be met.

(2) All bus voltages and branch currents in the network are restricted by Eq. (10) and Eq. (11), separately.

$$V_{min} \le V_i \le V_{max} \quad (10)$$

$$I_{min} \le I_i \le I_{max} \quad (11)$$

where, the maximum and minimum voltages are set to 1.05 p.u and 0.9 p.u.

(3) The penetration limits of distributed generators and capacitors are as follows:

$$\sum_{i=1}^{N_{DG}} P_{DG,i} \le 0.75 \sum_{i=1}^{N} P_{Li} \quad (12)$$

$$\sum_{i=1}^{N_{SC}} Q_{SC,i} \le 0.75 \sum_{i=1}^{N} Q_{Li} \quad (13)$$

where, N_{DG} and N_{SC} are the number of distributed generators and shunt capacitors, separately. $P_{DG,i}$ and $Q_{SC,i}$ represent the real power injected by DGs and reactive power by SCs at bus i, respectively. And the total size of DGs (or SCs) does not exceed 75% of the sum of load power in a system.

(4) System power factor limit: system power factor is limited to a range, as follows:

$$pf_{min} \le pf \le pf_{max} \quad (14)$$

where, the maximum and the minimum of power factors are represented by pf_{max} and pf_{min}, respectively, which are 0.8 and 0.95. The power factor of DGs can be set to 1. That is to say that DGs emit active power merely.

III. Algorithm Improvement

A. Butterfly Algorithm (BF)

Butterfly algorithm (BF) is a particle swarm optimization algorithm based on butterfly learning, inspired by intelligent behaviors, communication network and information exchange among butterfly groups in the process of collecting nectar [23]. Correspondingly, certain new parameters such as butterfly sensitivity (s), nectar probability (p) and node degree are introduced in the Butterfly algorithm.

The position of nectar represents the optimal solution to the optimization problem, and the amount of nectar represents the corresponding fitness value. Each butterfly continuously adjusts its flight gesture based on the best experience of itself and its neighbors. In the BF algorithm, the sensitivity and nectar probability in the search process determine the flight speed and position of the butterfly, and their ranges are both [0,1].

The values of sensitivity and nectar probability of butterflies are calculated iteratively according to the following equations.

$$s_k = \exp(-(C_{max} - C_k) / C_{max}) \quad (15)$$

$$p_k = Fit_{gbest,k} / \sum Fit_{lbest,k} \quad (16)$$

where, C_{max} is the maximum number of iterations, and C_k represents the k-th iteration. $Fit_{gbest,k}$ and $Fit_{lbest,k}$ represent the optimal fitness value and local best fitness value vector after k iteration, separately.

Eq. (15) contains the speed inertia weight coefficient w_k as follows:

$$w_k = (C_{max} - C_k) / C_{max} \quad (17)$$

The velocity iteration and position iteration equations are given in Eq. (18) and Eq. (19), respectively.

$$\begin{aligned} v_k = {} & k_1 w_k v_{k-1} + s_k (1 - p_k) c_1 r_1 (x_{lbest,k-1} - x_{k-1}) \\ & + p_g c_2 r_2 (x_{gbest,k-1} - x_{k-1}) \end{aligned} \quad (18)$$

$$x_k = x_{k-1} + \alpha_k \cdot v_k \quad (19)$$

where, v_k and x_k are the velocity vector and position vector of the k-th iteration of the population, respectively. c_1 and c_2 both represent acceleration coefficients. r_1 and r_2 are random numbers from 0 to 1. The global best probability is P_g, usually set to 1. α_k is the time-varying probability coefficient, and its value equals P_k multiplied by a random number. k_1 is a constant coefficient of 1.

Hence, the individual butterfly in the BF algorithm includes the locations and capacity information of DGs and SCs. As is shown in Eq. (20).

$$X_i = [l_{D,1}, ..., l_{D,ND}, l_{S,1}, ..., l_{S,NS}, P_1, ..., P_{ND}, Q_1, ..., Q_{NS}] \quad (20)$$

where, $l_{D,ND}$ is the installation position of the DGs ND, and $l_{S,NS}$ is the configuration location of the SCs NS. P_{ND} and Q_{NS} represent the capacity and DGs SCs, respectively.

The overall population of butterflies is represented by a matrix containing N individuals shown as Eq. (21).

$$X = [X_1, X_2, X_3, ..., X_N] \quad (21)$$

B. Improved BF Algorithm

The historical information of the individual butterfly itself and other individuals is represented by acceleration coefficient c_1 and c_2, which reflects the inheritance of individual information and the information exchange within the population. Thus, the size of c_1 and c_2 will have a great impact on the optimization speed and the accuracy of the results. For instance, the individual will stay in the local area for a long time if c_1 is too large. The result may fall into a local optimum when c_2 is too large. The constriction factor is introduced on the basis of BF forming the BF-CF algorithm, which allows the speed of individuals to be controlled effectively, to achieve a balance between local search and global search. The constriction factor calculation formula is as follows [17].

$$\zeta = \frac{2}{2 - c - \sqrt{c^2 - 4c}}, \quad c = c_1 + c_2 \quad (22)$$

The updated speed iteration formula is shown as Eq. (23). The location update formula has not changed.

$$\begin{aligned} v_k = {} & w_k v_{k-1} + \zeta (s_k (1 - p_k) c_1 r_1 (x_{lbest,k-1} - x_{k-1}) \\ & + c_2 r_2 (x_{gbest,k-1} - x_{k-1})) \end{aligned} \quad (23)$$

The position and speed of individual are strictly limited within a certain range throughout the procedure of optimizing, which are shown in Eq. (24) and Eq. (25).

$$|v_k| \le v_{max} \tag{24}$$

$$|x_k| \le x_{max} \tag{25}$$

C. Algorithm Implementation

In this paper, the installation nodes of DGs and SCs will be processed before using the BF-CF algorithm for optimization. The values of *LPI*, calculated by Eq. (9), are sorted in descending order. Then, the voltage value of each bus in the original system is calculated by the method of Newton Raphson, arranged in ascending order. Finally, a candidate node vector is obtained considering the *PLI* and the voltage sequence simultaneously. Those buses with higher *PLI* value and lower voltage amplitude are more likely to be selected as candidate nodes [9]. This process can significantly improve the optimization speed of the algorithm, with ensuring the accuracy of the optimization results.

```
begin
calculate LPI values, node voltages,
        candidate buses sequence is obtained;
1. input: control parameters (N, Cmax, c1, c2 );
2.      target function (PT, QT, or VD)
3.      initialize the population X;
4.      calculate target fitness values and constraint
          violation by Newton-Raphson method;
5.      record the initial Pbest[…];
6.      initial Gbest = min (Pbest)
7.      Ck = 1
8.      while Ck < Cmax
9.          update the location (X) of each individual base on
              Eq. (21), Eq. (19), Eq. (24) and Eq. (25);
10.         for i = 1: D (population size)
11.             constraints computation and processing;
12.             calculate current_Pbest[…];
13.             index = find (current_Pbest < Pbest);
14.             Pbest(: , index) = current_Pbest (:, index);
15.             current_Gbest = min (Pbest);
16.             if current_Gbest < Gbest
17.              Gbest = current_Gbest
18.             end if
19.         end for
20.         Ck = Ck +1
21.     end while
22. output: Gbest solution;
end
```

Fig. 2 Pseudo code of BF-CF algorithm

In this paper, the population size is set to 30. The butterfly population X is a matrix composed of 30 vectors of the X_i in BF-CF algorithm. The population of butterflies is initialized within constraints. Global optimal individual and local optimal individual are represented by *Gbest* and *Pbest*, respectively. The pseudo code and the flow diagram of the BF-CF algorithm are shown in Fig. 2 and Fig. 3, separately.

In general, the simulation work of this paper mainly includes two parts. In the first part, buses are processed combining *PLI* and voltage amplitude. The proposed improved BF-CF algorithm is applied to optimize locations and capacities of DGs and SCs in the second part. The optimization process is guided by the processed nodes, simplifying the search space and speeding up the search. The constriction factor is introduced in the algorithm to balance global optimization and local optimization, which will obtain search results of higher quality.

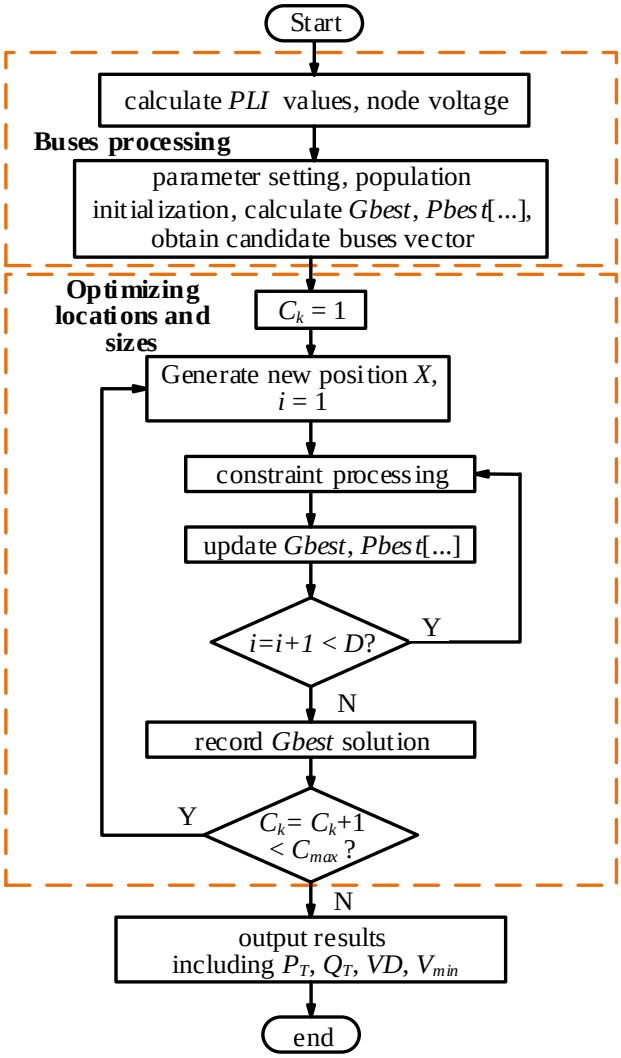

Fig. 3 Flow diagram of algorithm

D. Algorithm Performance Test

Using performance test function to verify the validity and rationality of the algorithm is one of the common methods. Here, six well-known test functions in TABLE I are used to test PSO, original BF and improved BF-CF respectively. Variable ranges of different test functions are also listed in TABLE I. In addition, several control experiments are set up to compare the advantages and disadvantages of different algorithms. Among them, the dimension of the six test function variables is 30, the number of variables is 50, and the maximum iteration is set to 500. The initial population and velocity are generated randomly.

For different test functions, each algorithm is tested for 20 times, and the minimum fitness values are taken for comparison. The fitness values of six test functions obtained by three algorithms can be observed in TABLE II. From the test results, the fitness values of the different test functions are the minimum by improved algorithm. Moreover, the comparison of the iterative curves of the three algorithms in Fig. 4 shows that the improved butterfly algorithm has the

TABLE I
SIX CONFESSED TEST FUNCTIONS

Test functions		Ranges
Sphere	$f_1(x)=\sum_{j=0}^{D} x_j^2$	[-100, 100]
Step	$f_2(x)=\sum_{j=0}^{D}(x_j+0.5)^2$	[-100, 100]
Schwefel 2.22	$f_3(x)=\sum_{j=1}^{D}\lvert x_j\rvert+\Pi_{j=1}^{D}\lvert x_j\rvert$	[-10, 10]
Schwefel	$f_4(x)=\sum_{j=1}^{D}-x_j\bullet\sin(\sqrt{\lvert x_j\rvert})$	[-500, 500]
Griewank	$f_5(x)=\sum_{j=1}^{D} x_j^2 \Big/ 4000-\Pi_{j=1}^{D}\cos(x_j/\sqrt{j})+1$	[-600, 600]
Ackley	$f_6(x)=-20\bullet e^{-0.2\bullet\sqrt{D^{-1}\bullet\sum_{j=1}^{D}x_j^2}}-e^{D^{-1}\bullet\sum_{j=1}^{D}\cos 2\pi\bullet x_j}+20+e$	[-32, 32]

TABLE II
THE FITNESS VALUES OBTAINED BY THREE ALGORITHMS THROUGH DIFFERENT TEST FUNCTIONS

Test functions	PSO	BF	BF-CF
Sphere	0.1406	0.0444	0.0025
Step	1.2463	0.6672	0.4505
Schwefel 2.22	2.7243	1.0038	0.4529
Schwefel	-7290.47	-6744.81	-7684.85
Griewank	1.0312	0.6981	0.5595
Ackley	1.9201	1.5573	0.9566

fastest optimization speed among the six test functions. The results above prove that our improvements on the original algorithm are effective and feasible.

IV. SYSTEMS AND TRIALS

The BF-CF algorithm is utilized to optimize the configuration of distributed generators and shunt capacitors in 33-bus, 69-bus and 119-bus radial networks, respectively. The data of loads and branches in 33-bus system and 69-bus system is obtained from [24]. The reference voltage and the reference capacity in standard test systems are set to 12.66 KV and 100 MVA, separately.

A. Original Systems

Calculating the *PLI* and the original bus voltage amplitude of test systems is for the purpose of obtaining the sequence of candidate buses.

a: 33-bus System

Fig. 5 is the structure diagram of the 33-bus system, which contains 32 branches. The total active load and the sum of reactive load are 3.175 MW and 2.3 MVAR, respectively. According to the power flow calculation results, the active power loss (P_T) and reactive power loss (Q_T) of the original system are 211 KW and 143.13 KVAR, separately.

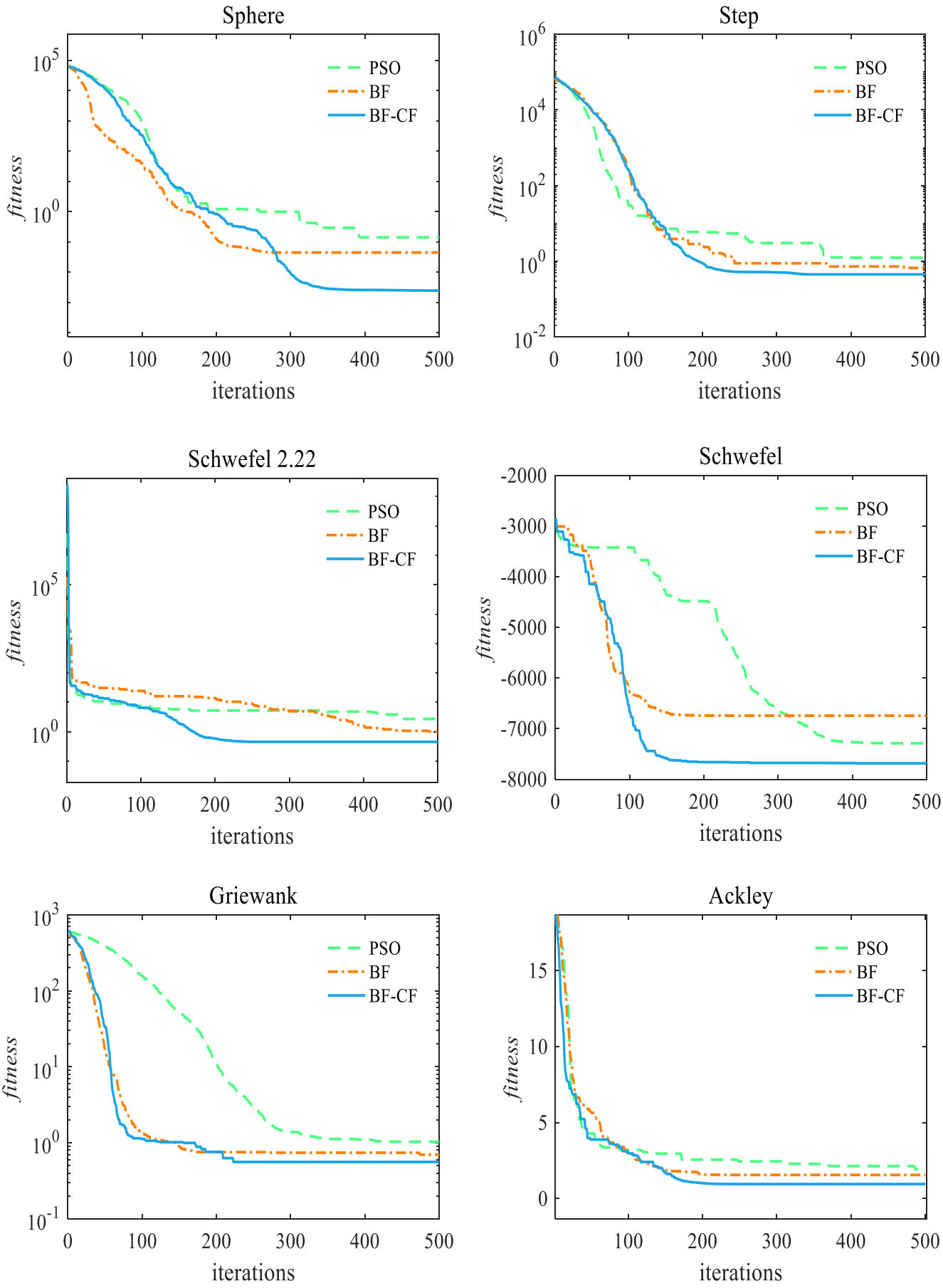

Fig. 4 Iterative graphs

The voltage distribution of the original 33-bus is shown in Fig. 6. It can be known from the figure that the maximum voltage is 1 p.u at first bus, the minimum voltage is 0.9038 p.u at bus 18 and the voltage deviation (*VD*) is 0.1338 p.u.

The value of *PLI* for each node calculated by Eq. (9) is shown in Fig. 7, in which *PLIDG* and *PLISC* have similar distribution trends. Nodes with higher *PLIDG* values include 7, 26, 30 and 6, etc. Among them, the maximum voltage is 1 p.u at the sixth node. Node 30 has the largest *PLISC*. Nodes with higher *PLISC* values also include 30, 29, 26 and 13, etc. These nodes with larger *PLI* and smaller voltage will be configured preferentially in the procedure of optimization for the 33-bus system.

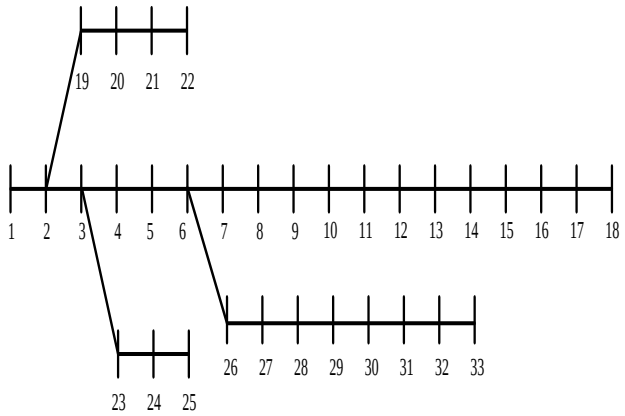

Fig. 5 33-bus system

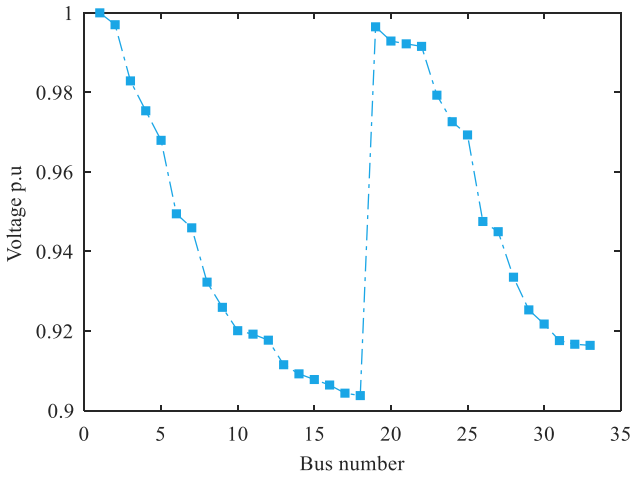

Fig. 6 Voltage profile of original 33-bus system

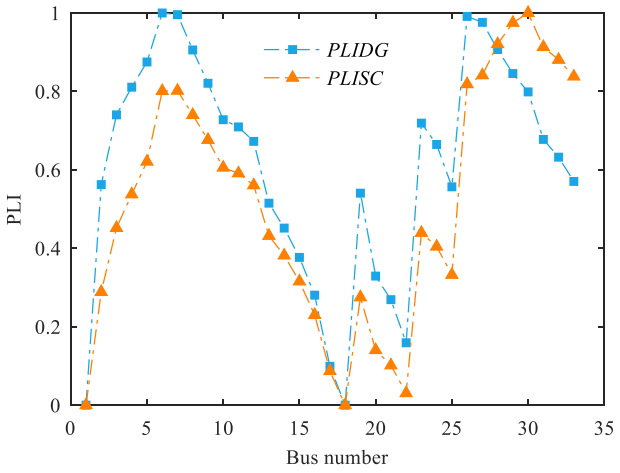

Fig. 7 Distribution of power loss index in 33-bus system

b: 69-bus System

The network structure diagram of the 69-bus system is detailed in Fig. 8 including 68 branches. The total loads are 3.792 MW and 2.694 MVAR. Bus voltage and power loss are gained by the method of Newton Raphson. The real power loss is 224.947 KW, the reactive power loss is 102.14 KVAR, and the voltage deviation is 0.0993 p.u.

Fig. 9 shows the voltage distribution of each node of the system. It can be seen from the figure that the maximum voltage is 1 p.u at the first bus and the minimum voltage is 0.9092 p.u at the 69th bus.

The power loss index distribution (*PLI*) of the 69-bus system is shown in Fig. 10. *PLIDG* and *PLISC* have similar distributions. Both the highest *PLIDG* and the highest *PLISC* are obtained at the 61st node. Buses with higher *PLI* contain bus 60, 62 and 11, etc. What is more, these nodes above all have lower voltage amplitude. Hence, these nodes are prioritized in the optimization process to reduce the optimization space.

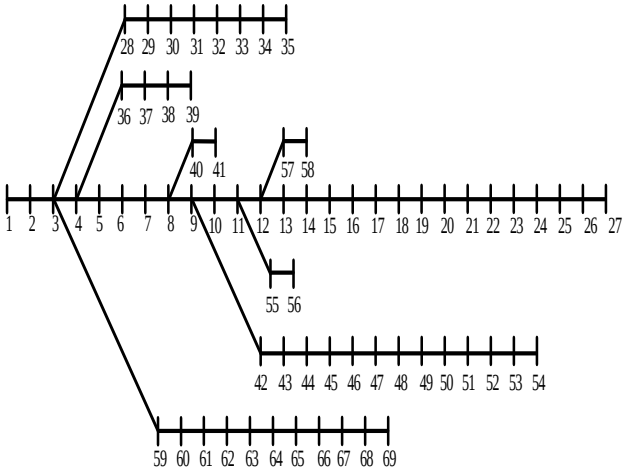

Fig. 8 69-bus system

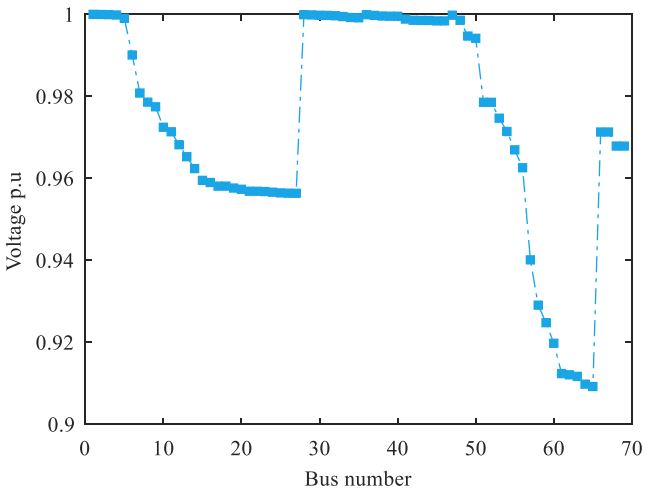

Fig. 9 Voltage profile of original 69-bus system

c: 119-bus System

The standard 12.66KV 119-bus distributed system contains 118 branches shown in Fig. 11. The total load power of the system is 22.71 MW and 17.041 MVAR. Base voltage and base power are set to 12.66 KV and 100 MVA, respectively.

The voltage profile of the system calculated by the power flow calculation is shown in Fig. 12, and its worst voltage and highest voltage are 0.9293 p.u at bus 113 and 1 p.u at the first node. The active power loss and reactive power loss of the original network are 978.1 KW and 718.8 KVAR, respectively. The voltage deviation is 0.1875 p.u.

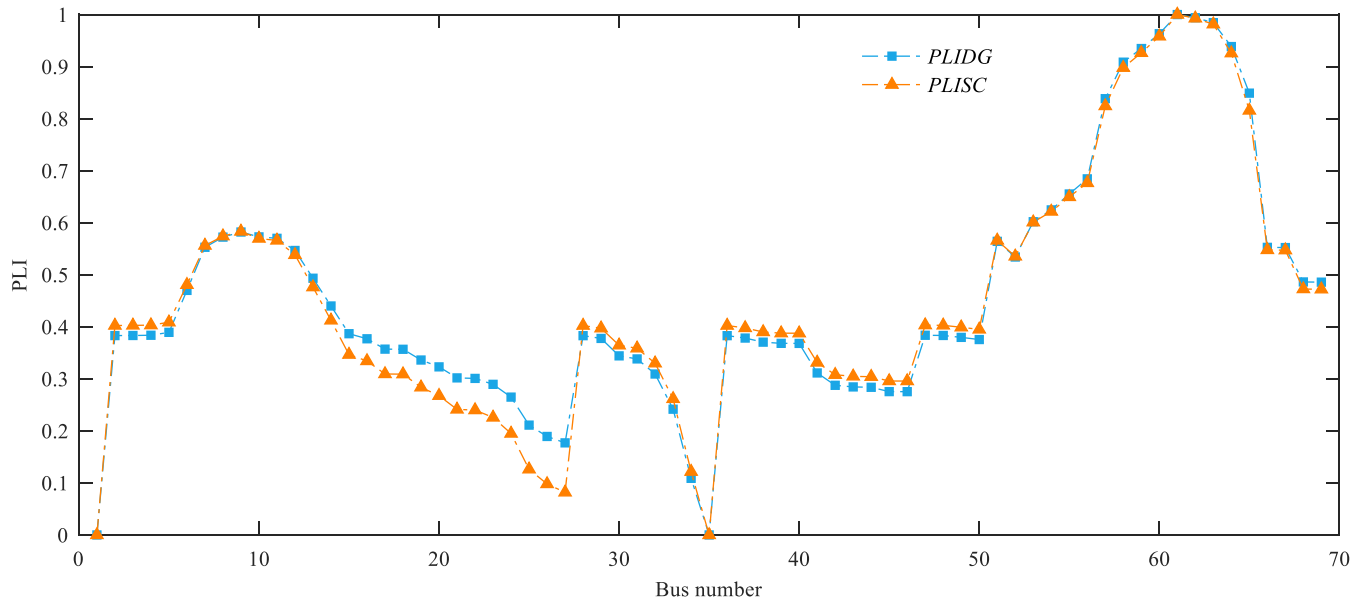

Fig. 10 Distribution of power loss index in 69-bus system

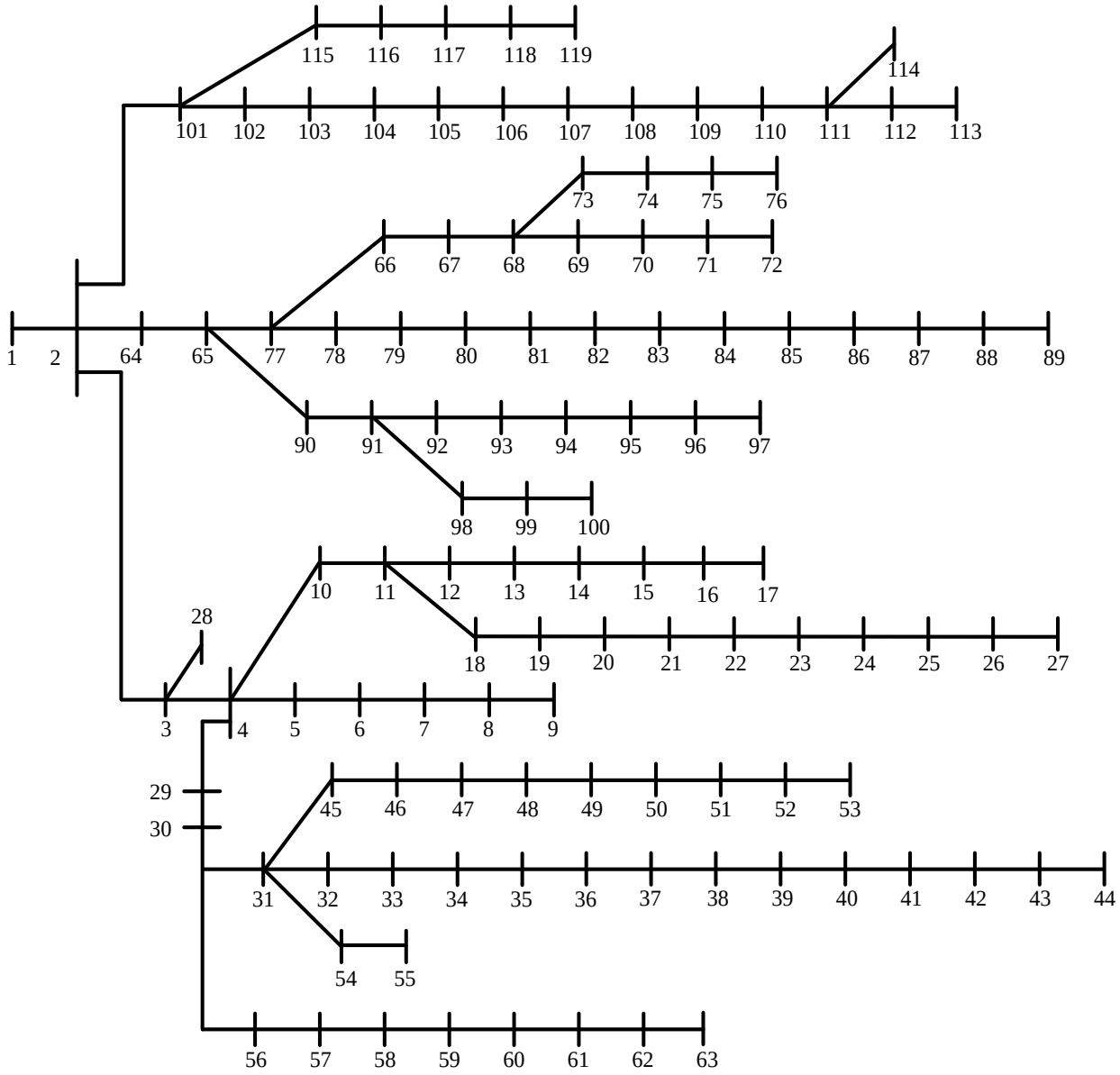

Fig. 11 119-bus system

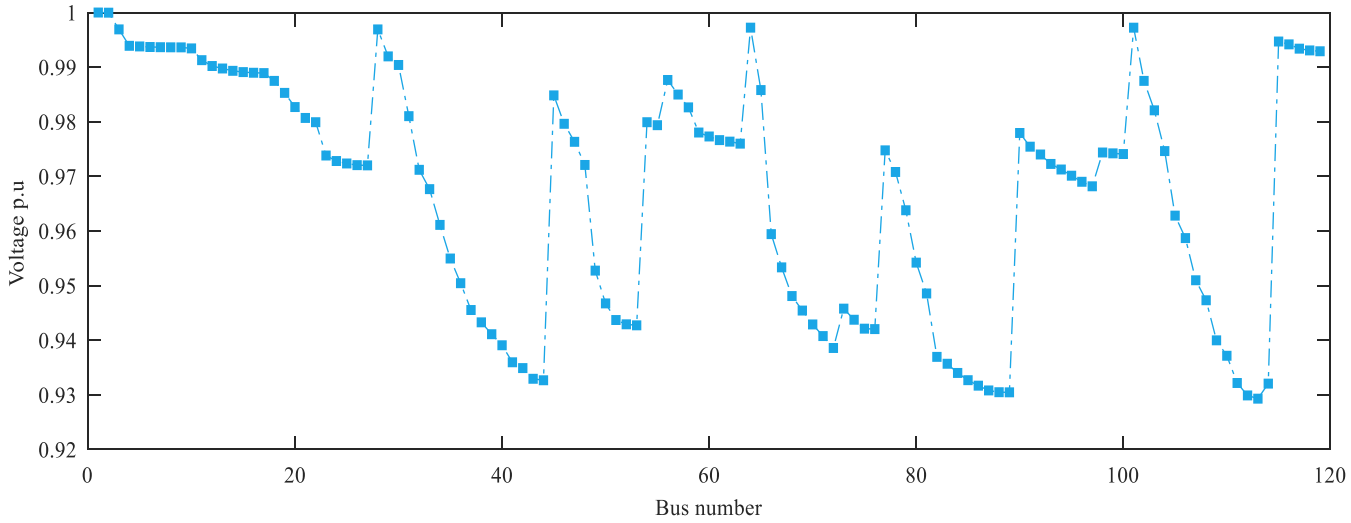

Fig. 12 Voltage profile of original 119-bus system

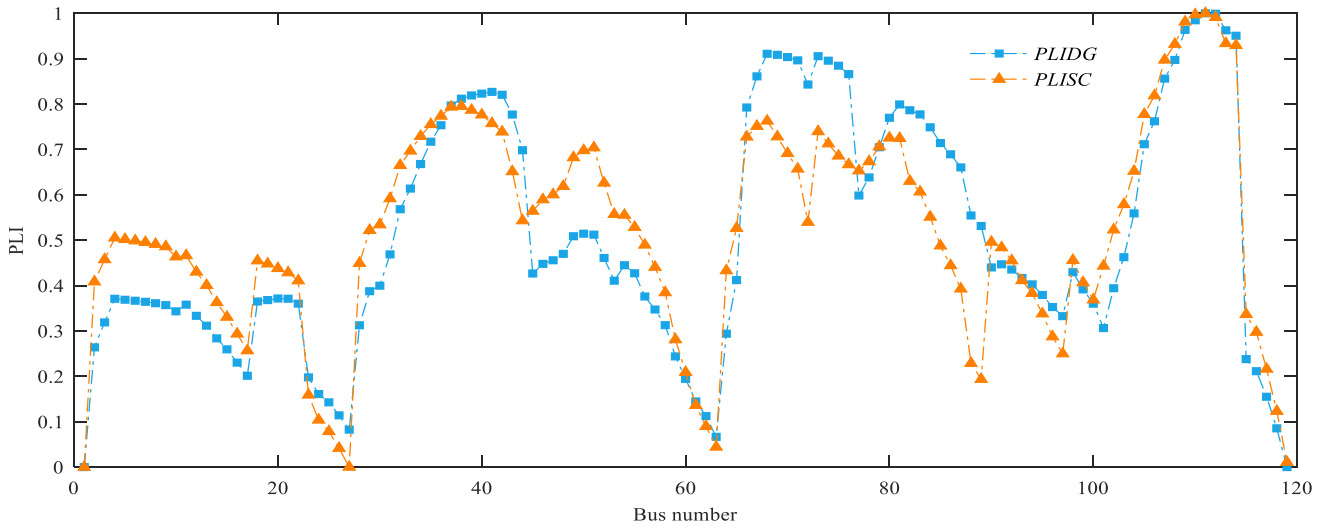

Fig. 13 Distribution of power loss index in 119-bus system

Obviously, compared with the 33-bus system and the 69-bus system, the 119-bus system has more nodes and a more complex structure. The *PLI* distribution curve of the system is shown in Fig. 13. The *PLI* values of nodes 111, 81, 73, and 40 are relatively large, and it is observed that the voltage amplitudes of these buses are relatively small from Fig. 12. In some complex systems with large scale such as the 119-bus system, that will significantly improve the optimization speed and search space of the intelligent algorithm. It will be verified in the simulation results below.

B. *Results and Discussion*

The capacity ranges of DGs and SCs installed in different standard test networks are calculated according to Eq. (12) and Eq. (13), as shown in TABLE III. This section records the simulation numerical results, voltage distribution and comparison of results for different cases of the three standard test systems in detail. 30 simulation experiments are carried out independently for each case of the three test systems to ensure the accuracy of the optimization results. The best results obtained by the BF-CF algorithm are compared with ones by other methods.

TABLE III
SIZE RANGE OF DGS AND SCS

Systems	Size range of DGs	Size range of SCs
33-bus	0-2.78MW	0-1.73MVAR
69-bus	0-2.84 MW	0-2.02 MVAR
119-bus	0-17.03 MW	0-12.78 MVAR

a: Results in 33-bus system

In order to verify the performance advantages of the BF-CF algorithm for configuring DGs and SCs in a small-scale power network, simulation cases from case 1 to case 9 are set up for the 33-bus system. Only SCs are configured in the first three cases. DGs are merely installed in case 4 to case 6, and DGs and SCs are optimized collectively in the last three cases.

TABLE IV details the simulation results of 9 cases of the 33-bus standard test system, including the location and capacity information of DGs and SCs, power loss P_T and Q_T, active loss reduction (*PPloss*) and reactive loss reduction (*QQloss*), and indicators such as the lowest voltage and voltage deviation of the system. It can be observed that the various indicators when only DGs are installed in the 33-bus system are significantly superior to those when only SCs are installed from in the three cases. For example, in case 3 (3 SCs), the active power loss and reactive power loss are 139.65 KW and 95.3 KVAR respectively. Compared with the original system, the active power loss is reduced by 33.82%,

TABLE IV
SIMULATION RESULTS OF 33-BUS SYSTEM

	case 1	case 2	case 3	case 4	case 5	case 6	case 7	Case 8	case 9
DGs size KW	-	-	-	2580(6)	852(13) 1147(30)	811(13) 1081(24) 1044(30)	2492(6)	843(13) 1148(30)	812(13) 821(25) 1012(30)
SCs size KVAR	1203(30)	465(12) 1048(30)	581(6) 302(14) 875(30)	-	-	-	1261(30)	449(12) 1056(30)	413(13) 411(25) 1026(30)
P_T (KW)	**151.46**	**141.85**	**139.65**	**111.02**	**87.17**	**72.76**	**58.47**	**28.5**	**12.62**
Q_T (KVAR)	103.85	96.49	95.3	81.67	59.78	50.65	47.04	20.41	10.06
PPloss (%)	28.22	32.77	33.82	47.38	58.69	65.52	72.29	86.49	94.02
QQloss (%)	27.44	32.58	33.41	42.94	58.23	64.61	67.13	85.74	92.97
V_{max} p.u	1(1)	1(1)	1(1)	1(1)	1(1)	1(1)	1(1)	1.0015(30)	1.0012(13)
V_{min} p.u	0.9161 (18)	0.9302 (18)	0.9325 (18)	0.9424 (18)	0.9682 (18)	0.9687 (33)	0.9534 (18)	0.9804 (25)	0.9921 (8)
VD p.u	0.0855	0.0639	0.0644	0.0377	0.0173	0.015	0.0174	0.0016	0.0007

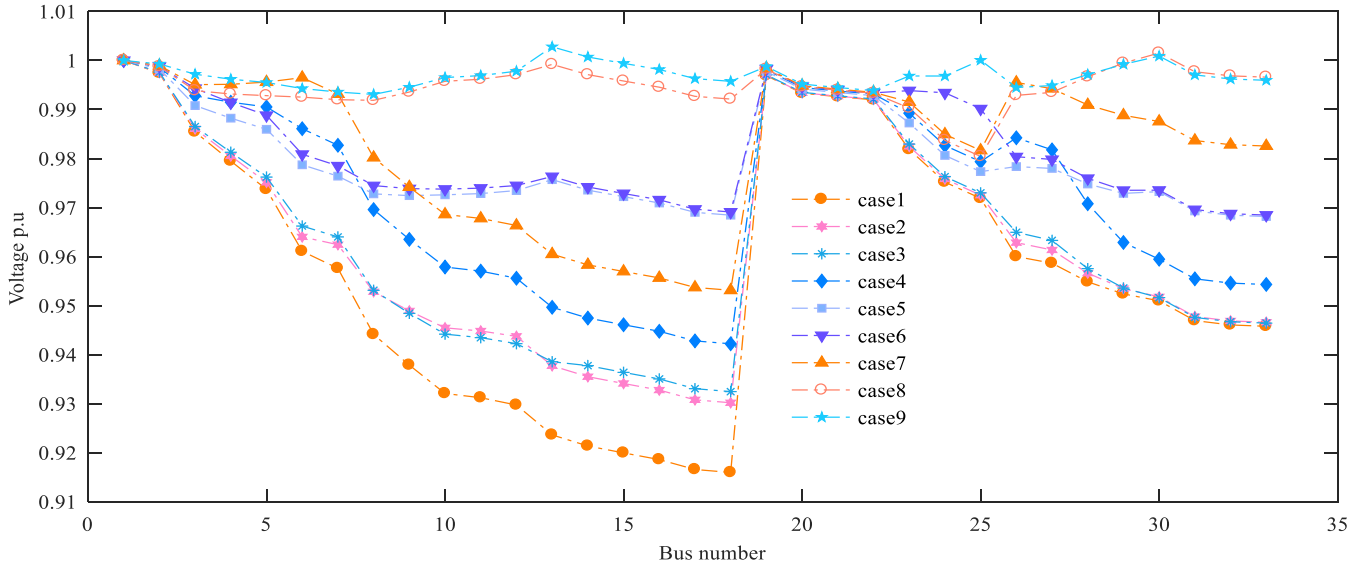

Fig. 14 Voltage profile for different case studies in 33-bus system

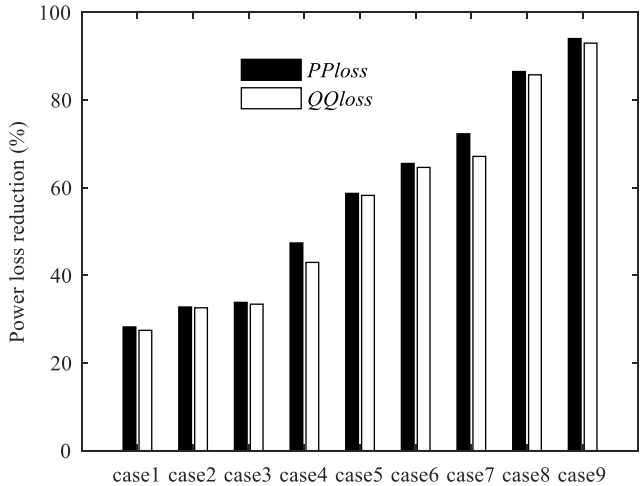

Fig. 15 Power loss reduction of each case in 33-bus system

and the reactive power loss is reduced by 33.41%. The lowest voltage is 0.9161 p.u at node 18, and the voltage deviation is 0.0644 p.u. In case 6(1 DGs), the active power loss and reactive power loss are significantly reduced to 72.76 KW and 50.65 KVAR, respectively. The power loss (P_T and Q_T) is reduced by 65.52% and 64.61%, and the worst voltage and voltage deviation are 0.9687 p.u and 0.015 p.u, respectively. The results from case 7 to case 9 indicate that the optimization results can be improved remarkably when DGs and SCs are configured at the same time. 3 DGs and 3 SCs are optimized simultaneously in case 9, and the real power loss is only 12.62 KW, which is a reduction of 94.02%. And the worst voltage is dramatically enhanced to 0.9921 p.u with voltage deviation of only 0.0007 p.u.

The percentage of active/reactive power loss reduction for each simulation case in the 33-bus system is shown in Fig. 15. It can be seen from case 1 to case 6 that the effect of configuring DGs solely is significantly better than that of configuring SCs alone. In case 5, the *PPloss* and *QQloss* are 58.69% and 58.23%, respectively, and the voltage deviation is only 0.0173 p.u, which are better than those in case 2. Optimized configuration of DGs and SCs at the same time can significantly reduce active power loss and reactive power loss. For example, in case 9 (with 3 DGs and 3 SCs), the *PPloss* and *QQloss* reach 94.02% and 92.97%, respectively.

It is worth noting that, in the 9 cases above, the installation positions of DGs and SCs have selected certain buses with larger *PLI* value and lower voltage value, such as nodes 6, 13, 30, which demonstrates that the processing of candidate nodes before is beneficial to the optimization results. What is the most important is that DGs and SCs are also installed at nodes 25 and 14 with lower power loss index, indicating that the positions configuration of DGs and SCs does not completely depend on the power loss index and voltage amplitude of the node, which verifies that the BF-CF algorithm has powerful global search capabilities.

In addition, installing DGs and SCs in the power system can also improve the voltage distribution of the system. Voltage distribution of 9 cases in the 33-bus system is presented in Fig. 14. Obviously, the voltage amplitude of the system is closer to the reference voltage as the number of DGs or SCs increases. In particular, the improvement of the system voltage distribution is very significant when DGs and SCs are configured at the same time. It can be observed from the figure that the voltage distribution in case 9 (with 3 DGs and 3 SCs) is closest to 1 p.u. Increasing the number of DGs and SCs units will lead the voltage of a few nodes in the system to exceed 1 p.u. For instance, the maximum node voltage is 1.0015 p.u in case 8, while all node voltages are within the allowable range set in this paper. More importantly, the voltage distribution of system has improved significantly.

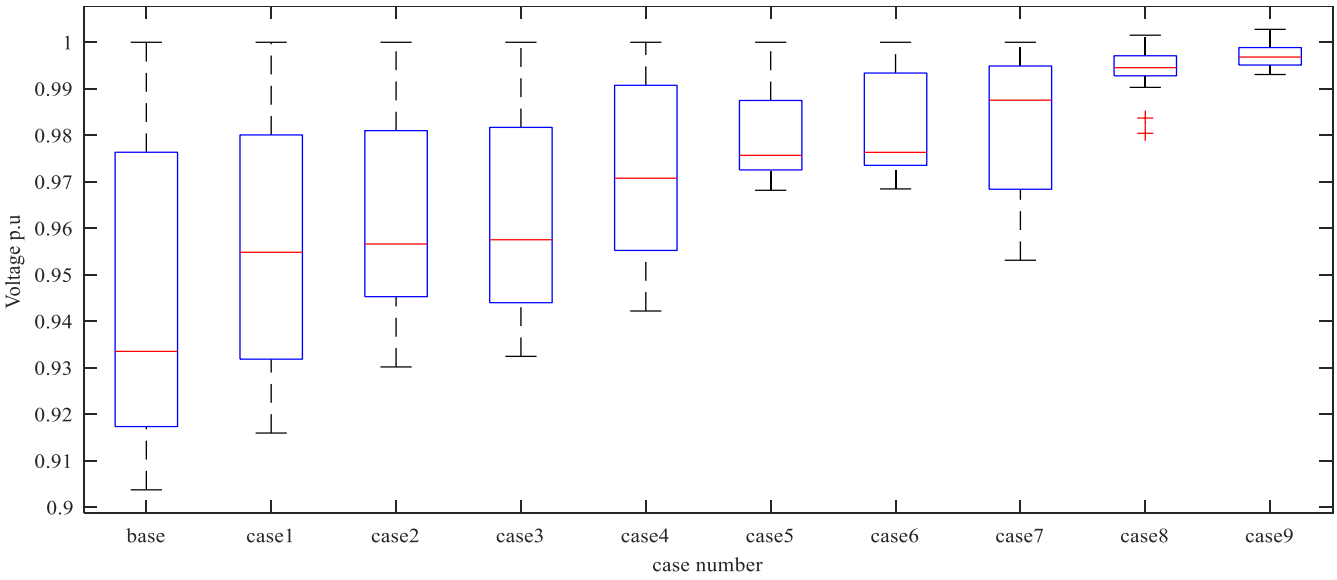

Fig. 16 Box plots of voltage for different case studies in 33-bus system.

TABLE V
RESULTS OF CERTAIN CASE STUDIES COMPARED WITH OTHER METHODS FOR 33-BUS SYSTEM

case	case 6 (3 DGs)	case 7 (1 DGs ,1SCs)	case 8 (2 DGs, 2SCs)	case 9 (3 DGs, 3 SCs)
parameter	P_T(KW) DGs size (KW) V_{min} (p.u)	P_T(KW) DGs size (KW) SCs size (KMVR) V_{min} (p.u)	P_T(KW) DGs size (KW) SCs size (KMVR) V_{min} (p.u)	P_T(KW) DGs size (KW) SCs size (KMVR) V_{min} (p.u)
proposed	**72.76** 811(13),1081(24) 1044(30) 0.9687(33)	**58.47** 2492(6) 1261(30) 0.9534(18)	**28.5** 843(13),1148(30) 449(12),1056(30) 0.9804(25)	**12.62** 812(13),821(25),1012(30) 413(13),411(25),1026(30) 0.9921(8)
BSOA[25]	89.05 632(13),487(28) 550(31) 0.9554(18)	-	-	-
PSO[26]	-	59.7 2511(6) 1457(30) 0.955(18)	-	-
MSSA[27]	-	-	29.15 817.6(13),1243.5(29) 359.4(15),1095.2(30) Not reported	-
IMDE[28]	-	-	32.08 1080(10),896.4(31) 254.8(16),932.3(30) 0.979(25)	-
EGA[29]	-	-	28.5 835.6(13),1161.7(30) 438.6(13),1047.4(30) 0.9804(25)	12.7 767.7(14),1094.9(27),964.2(30) 334.7(14),388.8(25),1189.9(30) 0.9924(8)

Comparing the voltage distribution in the simulation cases in Fig. 16 with those in the original system, it is found that the voltage distribution of the system in case 9 is the most concentrated with the highest average voltage.

The simulation results of case 6 to case 9 are compared with other intelligent algorithms in TABLE V, to verify the superiority of the proposed algorithm. When 3 DGs are installed in the system merely, the active power loss of the BF-CF algorithm is 72.26 KW, which is significantly lower than that of 89.76 KW obtained by the BSOA algorithm [25]. DGs and SCs are installed at node 6 and 30 both in PSO [26] and BF-CF, respectively. The active power loss of the former is 59.7 KW, and the worst voltage is 0.955 p.u. The active power loss of the latter is 58.47 KW, and the minimum voltage is 0.9534 p.u. In case 8, the positions of DGs and SCs in BF-CF are different from other three algorithms. The active power loss and the worst voltage obtained by the proposed algorithm are superior to those in MSSA [27] and IMDE [28], which are the same as the results by the EGA algorithm [29]. When 3 DGs and 3 SCs are configured jointly, real power loss in BF-CF is smaller than that in EGA, but the minimum voltage is slightly worse.

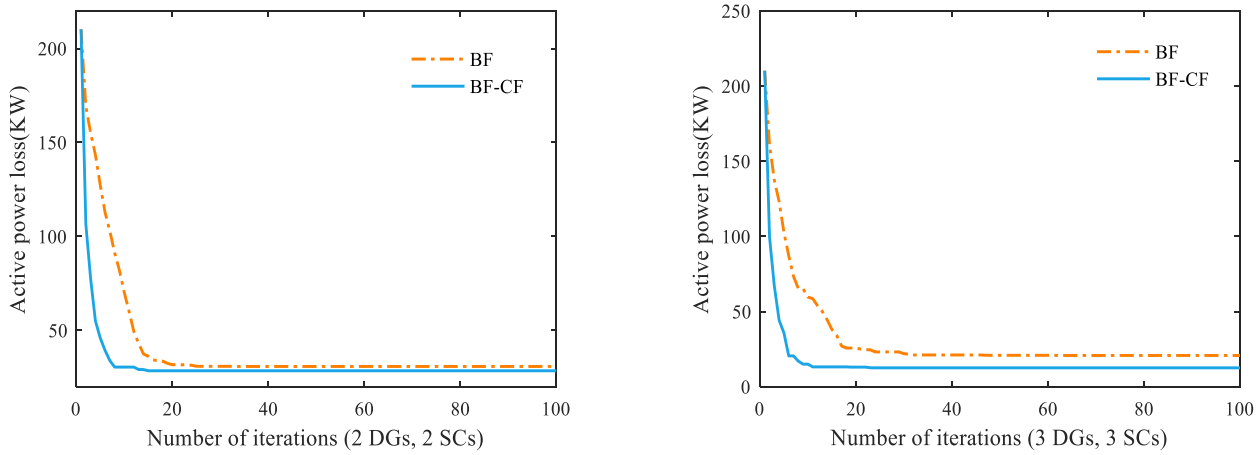

Fig. 17 Iterative curves of active power loss in 33-bus system

TABLE VI
SIMULATION RESULTS OF 69-BUS SYSTEM

	case 10	case 11	case 12	case 13	case 14	case 15	case 16
DGs size KW	-	-	457(20) 1906(61)	563(11),373(18) 1731(61)	1820(61)	527(18) 1729(61)	541(11),372(18) 1669(61)
SCs size KVAR	357(18) 1345(61)	521(9),295(18) 1208(61)	-	-	1295(61)	356(17) 1234(61)	413(11),232(21) 1196(61)
P_T(KW)	**146.6**	**145.32**	**72.47**	**69.41**	**23.13**	**7.19**	**4.28**
Q_T(KVAR)	68.3	67.71	36.21	34.94	14.38	8.04	6.74
PPloss (%)	34.82	35.38	67.78	69.14	89.72	96.80	98.10
QQloss (%)	33.10	33.68	64.53	65.78	85.92	92.13	93.40
V_{max} (p.u)	1(1)	1(1)	1(1)	1(1)	1(1)	1(1)	1.0005(11)
V_{min} (p.u)	0.9322 (65)	0.9316 (65)	0.9827 (65)	0.9796 (65)	0.9724 (27)	0.9942 (50)	0.9943 (50)
VD (p.u)	0.0559	0.0555	0.0054	0.0048	0.0119	0.0004	0.0001

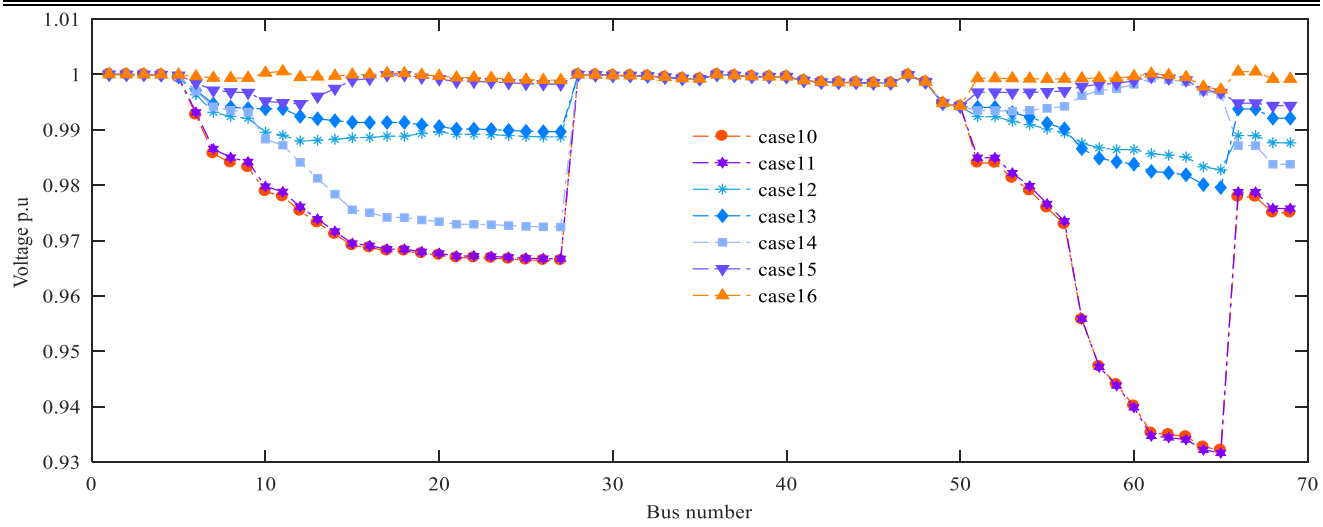

Fig. 18 Voltage profile for different case studies in 69-bus system.

The iterative curves of active power loss obtained by the BF and BF-CF algorithms are shown in Fig. 17. Compared with the original butterfly algorithm, the improved algorithm in this paper has faster convergence speed and better search results.

In summary, the BF-CF algorithm proposed in this paper can solve the problem of configuring DGs and SCs in the 33-bus system effectively.

b: Results in 69-bus system

The results of 7 case studies in the 69-bus system are listed in TABLE VI. From the results in the table, it is observed that configuring DGs and SCs in 69-bus system appropriately can boost the indicator of active power loss significantly. Similar to the simulation results of 33-bus system, the system performance improvement by configuring DGs or SCs alone is far less than that by configuring DGs and SCs jointly. In case 13, DGs are placed at node 11, 18 and 61, resulting in real power loss of 69.41 KW, reactive power loss of 34.94 KVAR and worst voltage of 0.9796 p.u. The system power loss (4.28 KW and 6.74 KVAR) of case 16 is superior to those in case 13. Compared with the original system, the active power loss and reactive power loss of the system are reduced by 98.1% and 93.4% respectively, and the worst voltage is 0.9943 p.u.

Furthermore, buses 61 and 11 with a higher *PLI* value and a lower voltage amplitude are selected as configuration positions for DGs and SCs. DGs and SCs are also installed on some buses such as 18 and 17 with lower *PLI*, further verifying the necessity of processing candidate nodes in the 69-bus system and the excellent global search capability of the BF-CF algorithm.

It can be seen from the Fig. 21 that configuring DGs and SCs in the 69-bus system at the same time can significantly reduce the power loss of the system and improve the performance of the system. Taking into account constraints of the actual situation and investment cost, the method of configuring DGs and SCs jointly is usually used to improve the performance indicators of the overall system.

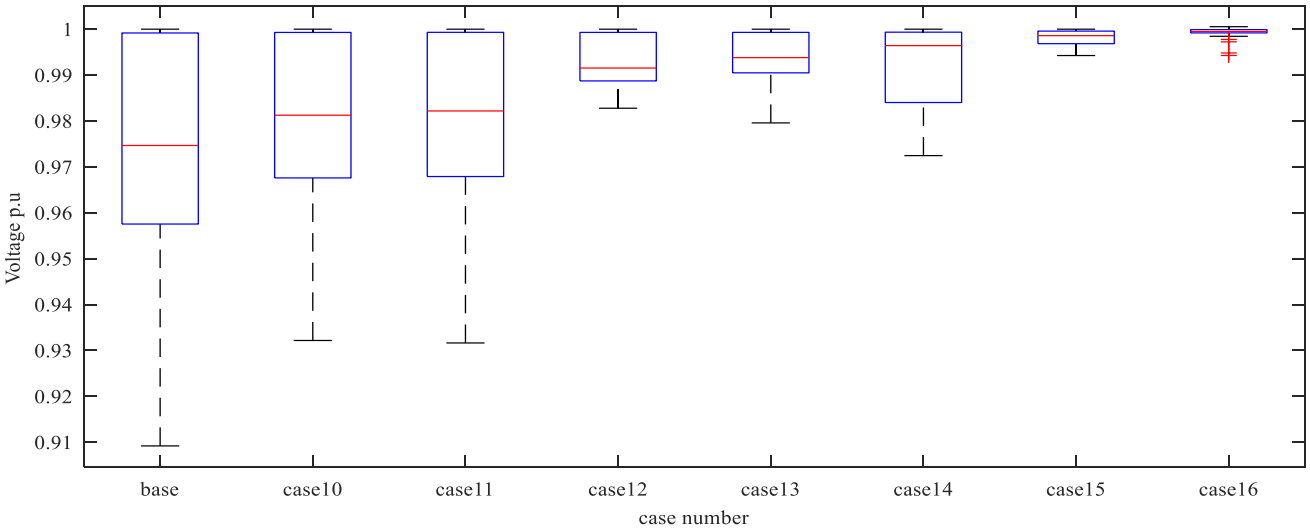

Fig. 19 Box plots of voltage for different case studies in 69-bus system

TABLE VII
RESULTS OF CERTAIN CASE STUDIES COMPARED WITH OTHER METHODS IN 69-BUS SYSTEM

case	case 11 (3 SCs)	case 13 (3 DGs)	case 14 (1 DGs, 1 SCs)	case 15 (2 DGs, 2 SCs)	case 16 (3 DGs, 3 SCs)
parameter	P_T(KW) SCs size (KMVR) V_{min} (p.u)	P_T(KW) DGs size (KW) V_{min} (p.u)	P_T(KW) DGs size (KW) SCs size (KMVR) V_{min} (p.u)	P_T(KW) DGs size (KW) SCs size (KMVR) V_{min} (p.u)	P_T(KW) DGs size (KW) SCs size (KMVR) V_{min} (p.u)
proposed	**145.32** 521(9),295(18) 1208(61) 0.9316(65)	**69.41** 563(11),373(18) 1731(61) 0.9827(65)	**23.13** 1820(61) 1295(61) 0.9724(27)	**7.19** 527(18),1729(61) 356(17),1234(61) 0.9942(50)	**4.28** 541(11),372(18),1669(61) 413(11),232(21),1196(61) 0.9943(50)
COA[30]	146.26 300(17),1500(57) 1208(61) 0.9313(65)	-	-	-	-
QOCSOS[31]	-	72.13 627(11),435(20) 1947(61) Not reported	-	-	-
MOEA/D[7]	-	-	23.17 1829(61) 1301(61) 0.9731(27)	7.20 520(17),1731(61) 353(17),1239(61) 0.9943(69)	-
IPSO[32]	-	-	-	-	4.37 557(11),321(21),1672(61) 300(11),300(18),1200(61) 0.9943(50)

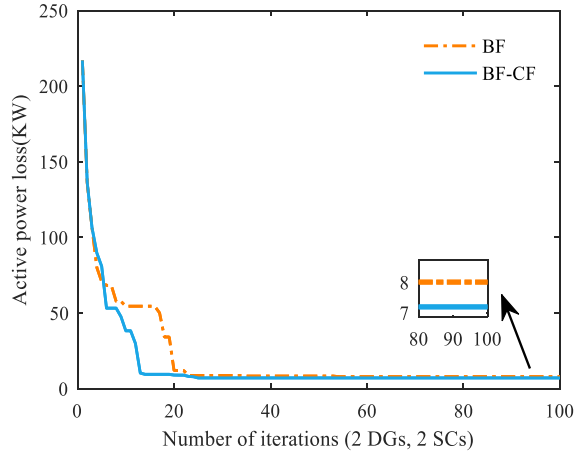

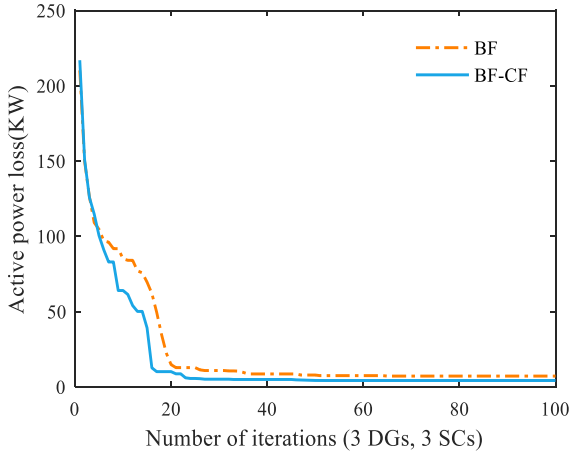

Fig. 20 Iterative curves of active power loss in 69-bus system

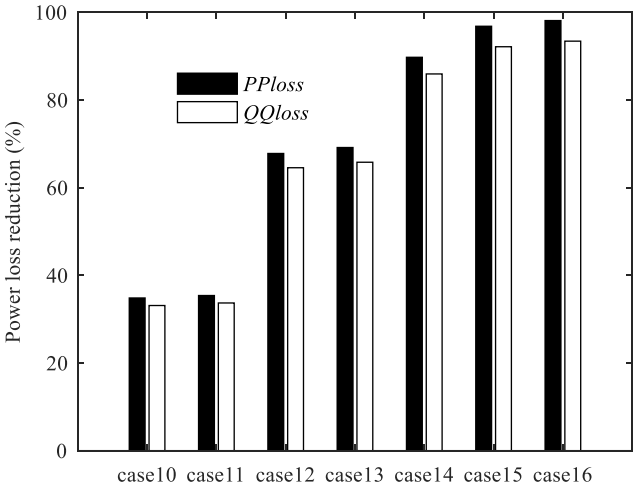

Fig. 21 Power loss reduction of each case in 69-bus system

From the voltage distribution of different simulation cases in Fig. 18 and Fig. 19, it can be known that the voltage distribution of the 69-bus system is enhanced dramatically by BF-CF and bus voltages in all cases are within the given range. The smoothest voltage curve and the most concentrated voltage distribution are in case 16.

TABLE VII compares the simulation results of case 11 and case 13 to case 16 with other methods. In case 11 and case 13, the values of actual power loss obtained by BF-CF are 145.32 KW and 69.41 KW, respectively, which are superior to 146.26 KW by COA in [30] and 72.13 KW by QOCSOS in [31]. Moreover, the search performance of the BF-CF algorithm is also better than other intelligent methods when DGs and SCs are configured simultaneously. In case 14 (with 1 DGs and SCs), the power loss and lowest voltage by BF-CF are 23.13 KW and 0.9724 p.u respectively, which are better than the power loss of 23.17 KW and the worst voltage of 0.9713 p.u obtained by MOEA/D [7]. The BF-CF algorithm is also more advantageous in optimizing multiple DGs and SCs at the same time. For example, in case 16 with 3 DGs and 3 SCs, the value of objective function is 4.28 KW, lower than the 4.37 KW obtained by IPSO [32].

The power loss iteration curves in Fig. 20 shows that the algorithm proposed in this paper has a faster convergence speed and smaller active power loss.

These comparisons indicate that the performance of the BF-CF method for configuring DGs and SCs in the 69-bus system is superior to other methods.

c: Results in 119-bus system

The above simulation results demonstrate that the algorithm proposed in this paper can effectively solve the problem of configuring DGs and SCs in the 33-bus system and 69-bus system. And compared with other intelligent algorithms, the results obtained by the BF-CF algorithm have higher quality. In the 119-bus system, multiple sets of simulation cases are set up the with minimum active power loss (P_T) and minimum voltage deviation (*VD*) as objectives, which is for the purpose of verifying the effectiveness of the method proposed in this paper in solving the DGs and SCs configuration problems in large-scale systems. The cases of configuring DGs and SCs jointly are studied considering the huge and complex structure of the 119-bus system.

(1) P_T as the objective

TABLE VIII lists positions and capacities of DGs and SCs obtained by BF-CF, BF and PSO for case 17 to case 21, separately, when the objective is minimum P_T. It is obtained from the table that nodes 111, 81, 38 and 73 with higher *PLI* are selected as sites of installation DGs and SCs in BF-CF, while the buses in BF and PSO are randomly selected by algorithms. Additionally, the total configuration capacity of DGs and SCs obtained by BF-CF is superior to those by other two methods.

The voltage distribution curves for 5 cases of the 119-bus system are shown in Fig. 22. Curves in the figure indicate that as the number of DGs and SCs increases, the voltage distribution of the network nodes is closer to the reference voltage value of 1 p.u. The smoothest voltage profile is gained in case 21 configuring 6 DGs and 6 SCs and the voltage distribution is the most concentrated shown as Fig. 23.

The simulation results of BF-CF in different studies are compared with those of BF and PSO in TABLE IX. It is worth noting that the objective values (P_T) obtained by BF-CF are superior to those gained by BF and PSO. The real power losses of these three algorithms are approximately 737 KW when 1 DGs and 1 SCs are considered in case 17. When 2 or 3 DGs and SCs are configured, the search results of BF-CF and BF are better than those in PSO. For example, the active power losses in case 18 obtained by BF-CF and BF are close to 574.09 KW, while the result by PSO is 591.96 KW. Additionally, compared with BF and PSO, the ascendancy of the BF-CF algorithm is more significant if the number of

TABLE VIII
CONFIGURATION INFORMATION OF DGS AND SCS IN 119-BUS SYSTEM FOR MINIMIZING P_T

Methods	Location & size	case 17 (1 DGs, 1 SCs)	case 18 (2 DGs, 2 SCs)	case 19 (3 DGs, 3 SCs)	case 20 (4 DGs, 4SCs)	case 21 (6 DGs,6 SCs)
BF-CF	DG size KW (bus)	2786(111)	2905(81) 2834(111)	3643(38),2900(81) 2869(111)	3309(40),3030(68) 2243(81),2906(111)	3037(40),1467(52) 2768(73),1816(84) 1083(96),2929(111)
	SC size KVAR (bus)	2364(111)	2068(81) 2367(111)	2705(38),2183(81) 2237(111)	2429(40),1914(68) 1697(81),2402(111)	2161(40),1614(52) 1782(73),1281(84) 671(96),2390(111)
BF	DG size KW (bus)	2876(111)	2877(81) 2837(111)	3342(40),2938(81) 2914(111)	3687(38),3127(68) 664(73),2937(111)	3307(40),1518(52) 1702(71),1701(85) 1809(98),2913(111)
	SC size KVAR (bus)	2309(111)	1994(81) 2301(111)	2410(40),2063(81) 2416(111)	2829(38),1275(68) 1103(73),2400(111)	2345(40),1587(52) 1678(73),1273(85) 1187(98),2446(111)
PSO	DG size KW (bus)	2856(111)	1945(85) 2875(111)	2818(42),1963(85) 2907(111)	3234(40),5263(64) 3177(73),2851(111)	2458(44),2479(51) 2768(71),1757(85) 1452(98),2979(111)
	SC size KVAR (bus)	2349(111)	1415(85) 2319(111)	2055(42),1449(85) 2418(111)	2281(40),3423(64) 2016(73),2387(111)	1835(44),1791(51) 429(71),1292(85) 1154(98),2564(111)

TABLE IX
RESULTS COMPARISON WITH BF AND PSO IN 119-BUS SYSTEM FOR MINIMIZING P_T BY BF-CF

Methods	parameters	base	case 17	case 18	case 19	case 20	case 21
BF-CF	P_T(KW)	978.10	**737.00**	**574.09**	**395.74**	**273.77**	**150.93**
	Q_T(KVAR)	718.80	586.9	458.70	266.77	190.53	104.77
	V_{max} (p.u)	1(1)	1(1)	1(1)	1.0031(38)	1.0028(40)	1.0035(84)
	V_{min} (p.u)	0.9293(113)	0.9305(89)	0.9326(44)	0.9471(53)	0.9467(53)	0.9735(27)
	VD (p.u)	0.1875	0.1518	0.0940	0.0492	0.0281	0.0094
BF	P_T(KW)	978.10	737.08	574.14	400.23	359.72	162.37
	Q_T(KVAR)	718.80	586.9	459.60	266.82	241.16	106.76
	V_{max} (p.u)	1(1)	1(1)	1(1)	1.0029(40)	1.0046(38)	1.0062(71)
	V_{min} (p.u)	0.9293(113)	0.9304(89)	0.9327(44)	0.9467(53)	0.9464(89)	0.9735(27)
	VD (p.u)	0.1875	0.1517	0.0946	0.0499	0.0507	**0.0087**
PSO	P_T(KW)	978.10	737.04	591.96	423.46	366.03	210.93
	Q_T(KVAR)	718.80	585.83	477.19	290.61	250.06	135.27
	V_{max} (p.u)	1(1)	1(1)	1(1)	1.0011(111)	1.0005(40)	1.0070(44)
	V_{min} (p.u)	0.9293(113)	0.9305(89)	0.9327(44)	0.9461(53)	0.9459(89)	0.9733(27)
	VD (p.u)	0.1875	0.1817	0.0979	0.0553	0.0528	0.0125

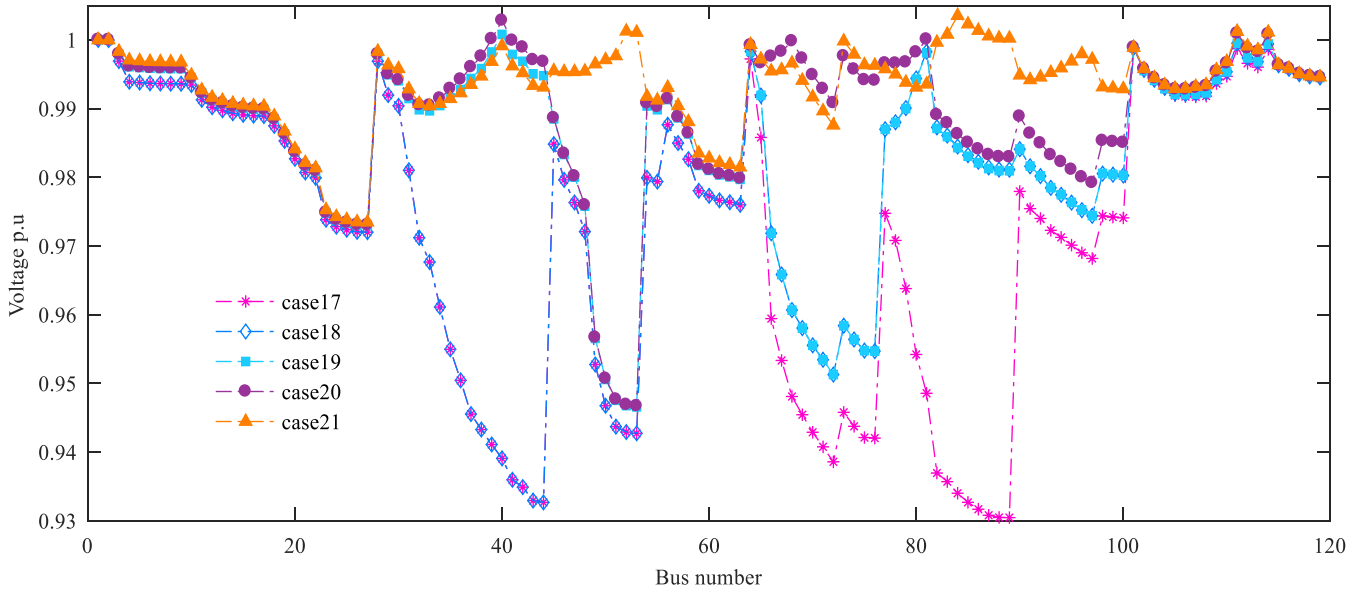

Fig. 22 Voltage profile for different case studies in 119-bus system for minimizing P_T by BF-CF

configuring DGs and SCs exceeds three. Especially in case 21, active power loss of 150.93 KW, reactive power loss of 104.77 MVAR, maximum voltage of 1.0035 p.u and worst voltage of 0.9735 p.u surpass those obtained by BF and PSO.

The percentage reduction of power loss obtained by BF-CF, BF and PSO algorithms is shown as Fig. 24. The results in Fig. 24 indicate that these three search algorithms can effectively cope with the problem of optimizing configuration of DGs and SCs in the 119-bus system. However, the real power loss and the reactive power loss

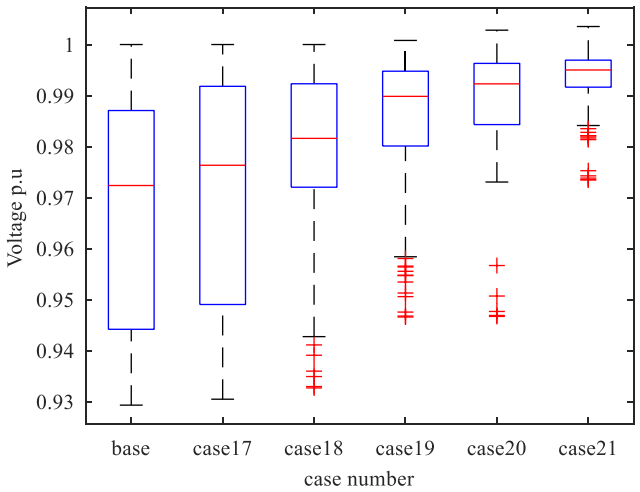

Fig. 23 Box plots of voltage in 119-bus system for minimizing P_T

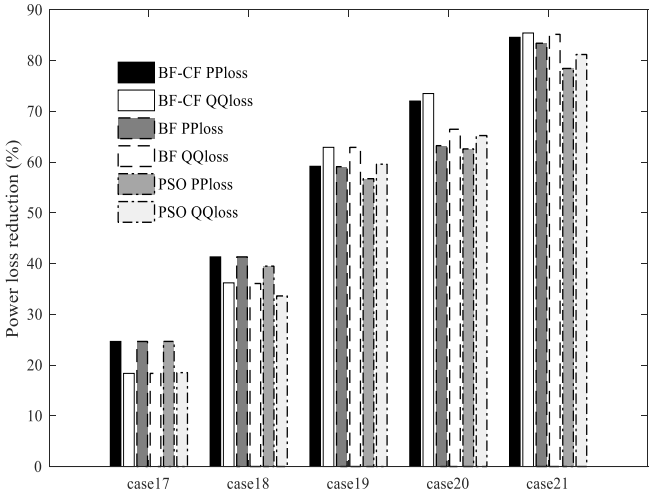

Fig. 24 Percentage of power loss reduction in 119-bus system for minimizing P_T

by the algorithm in this paper are superior to those obtained by BF and PSO. Especially in case 20, *PPloss* and *QQloss* obtained by BF-CF are lower than the results of BF and PSO by about 14%.

Convergence speed characteristics of BF-CF, BF and PSO targeting with minimizing active power loss are presented in Fig. 25. As can be seen from the figure, when the number of DGs and SCs both exceed 3, the algorithm proposed in this paper has conspicuous advantages in convergence speed and search results among different cases.

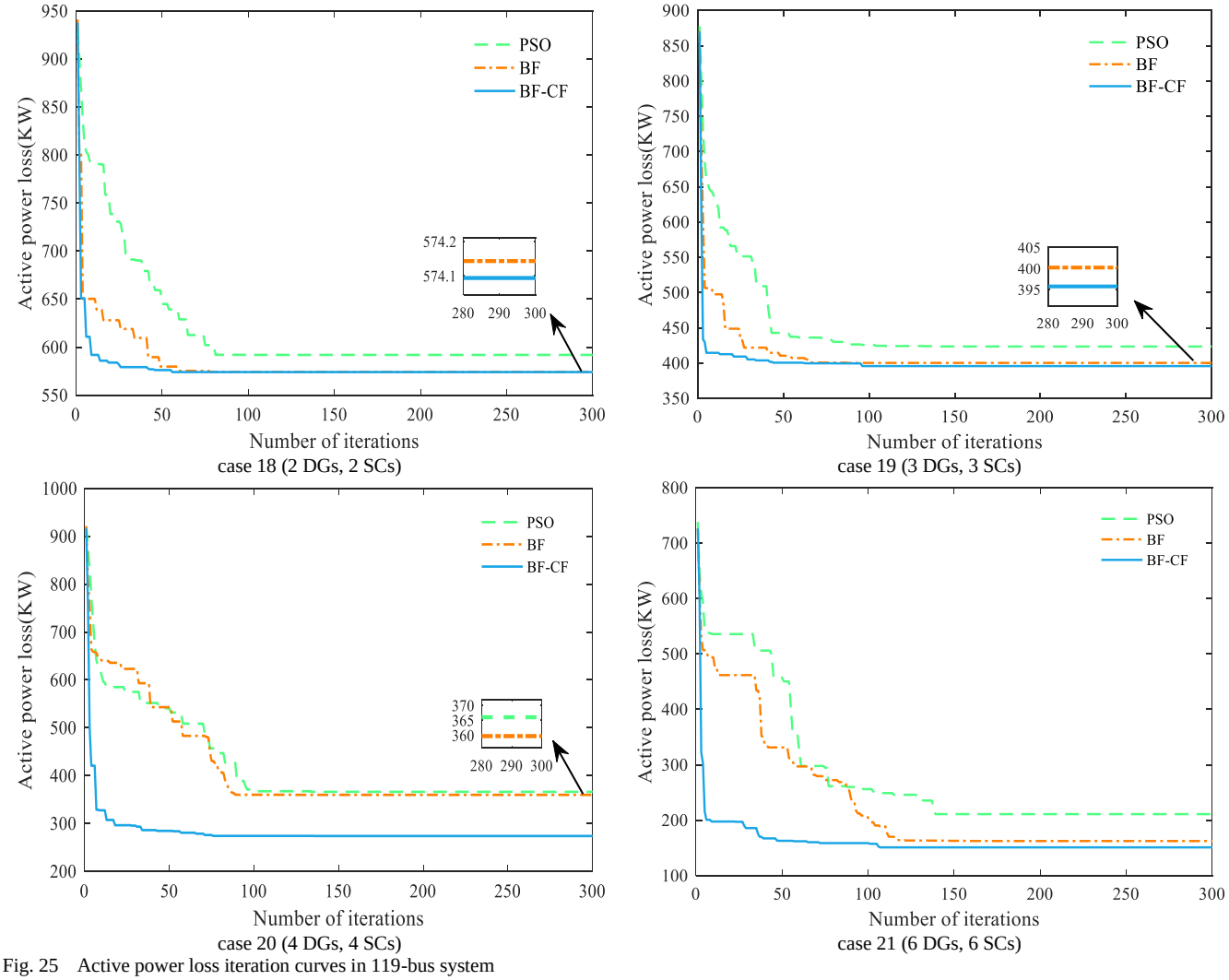

Fig. 25 Active power loss iteration curves in 119-bus system

In case 21, PSO achieves convergence within 136 iterations with real power loss of 210.93 KW, and the active power converges to 162.37 KW after 129 iterations in BF. While in the BF-CF algorithm, the curve of active power loss converges to 150.93 KW after only 106 iterations.

TABLE X lists the average value and standard deviation of the active power loss of the three algorithms running independently 30 times. Obviously, the mean and standard deviation obtained by BF-CF are better than the other two algorithms.

TABLE X
THE AVERAGE VALUE AND STANDARD DEVIATION OF THE *PT* (KW) IN 119-BUS SYSTEM

case	PSO		BF		BF-CF	
	mean	std	mean	std	mean	std
case 17	737.17	0.000668	737.22	0.000659	737.06	7.87E-05
case 18	592.04	0.000138	574.41	0.000225	574.36	0.000138
case 19	423.59	0.001315	401.87	0.000374	396.28	0.001251
case 20	366.98	0.001068	362.00	0.003667	280.29	0.031021
case 21	211.07	0.033030	163.27	0.006041	152.81	0.001603

Through the comparative analysis above, when minimum P_T as the objective, it is concluded that the BF-CF algorithm is a very effective method for solving the DGs and SCs configuration problems in the 119-bus system. A smaller active power loss value and superior reference target values can always be obtained by the method of BF-CF. Furthermore, the BF-CF algorithm has a faster convergence speed than BF and PSO, which certificates the convergence speed and robustness of the algorithm.

(2) VD as the objective

When the minimum *VD* is taken as the target, the configuration information of DGs and SCs obtained by PSO, BF, and BF-CF are listed in TABLE XI. Apparently, when configuring DGs and SCs using the method proposed in this paper, certain nodes with high *PLI* value and low voltage value are selected as installation locations, such as nodes 111, 81, 68 and 38. In case21a, node 50 is also selected as the installation node for DGs and SCs. This is because the constriction factor is introduced in BF-CF, which enables algorithm to take into account both global search and local search, so the installation node may also be a non-candidate node. When the original BF algorithm and PSO algorithm configure the installation positions of DGs and SCs, there is no candidate nodes vector to guide, so installing nodes are selected randomly.

TABLE XII lists the solution results of the three algorithms PSO, BF and BF-CF when the optimization objective is the minimum voltage deviation. According to the results in the table, it can be seen that the more DGs and SCs are configured in the 119-bus system, the better the optimization effect obtained by the method proposed in this paper. In case 17a with 1 DGs and 1 SCs, the values of minimum voltage deviation obtained by PSO and BF both are 0.1516 p.u, which is inferior to the result (0.1515 p.u) obtained by BF-CF. When there are multiple DGs and SCs considered simultaneously, the solution of the proposed method has higher quality. For instance, in case 20a (4 DGs and 4 SCs), the minimum voltage deviation and minimum voltage obtained by the BF-CF algorithm are 0.0246 p.u and 0.9477 p.u respectively, which are superior to 0.0256 p.u, 0.9469 p.u by PSO and 0.0257 p.u, 0.9469 p.u by BF. It is worth noting that in case 21a, the minimum voltage deviation of the objective function value and the minimum active power loss of the reference index by BF-CF are better than the other two algorithms (PSO and BF), which are 0.0079 p.u and 158.23 KW respectively.

Fig. 28 is the voltage distribution curve obtained by 5 simulations from case 17a to case 21a. The distribution curves in the figure indicate that the proposed method can effectively improve the overall voltage performance of the 119-bus system when the objective function is the minimum voltage deviation. In particular, case 21a has the smoothest voltage distribution, and the system voltage performance is improved dramatically, which is also verified by the voltage box plots shown in Fig. 26. From the perspective of system voltage distribution, the voltage value of some nodes exceeds the reference voltage value, but they are all within the voltage limit range. The BF-CF algorithm improves the system's voltage deviation and worst voltage significantly.

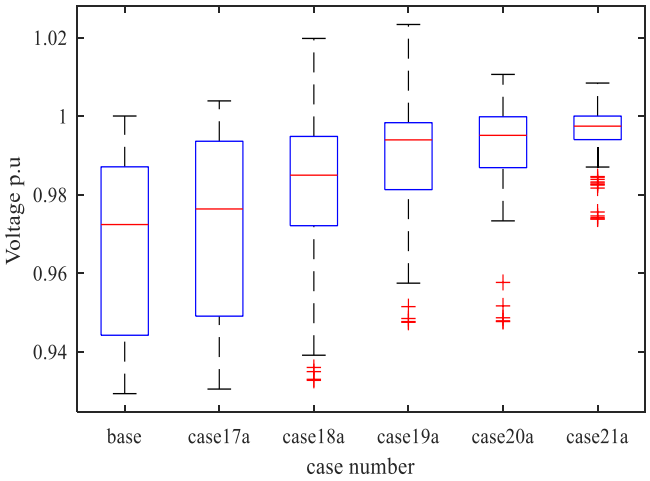

Fig. 26 Box plots of voltage in 119-bus system for minimizing *VD*

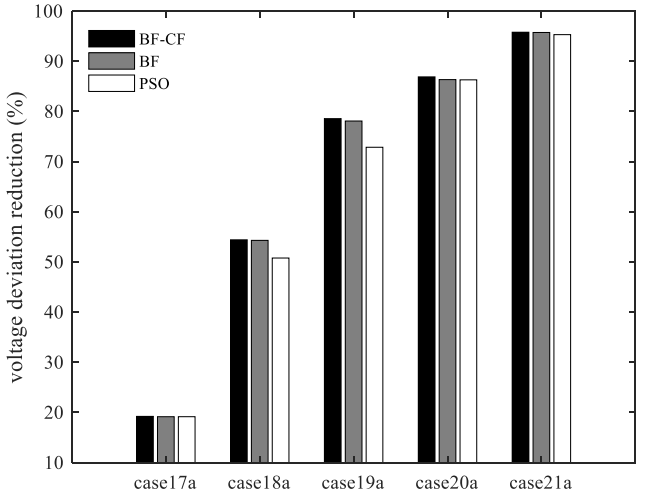

Fig. 27 Percentage of voltage deviation reduction in 119-bus system for minimizing *VD*

Fig. 27 lists the voltage deviation reduction percentages obtained by PSO, BF and BF-CF. These three algorithms all reduce the voltage deviation of the system to varying degrees. In the 5 simulation cases, the optimization results of BF-CF are better than those obtained by the other two algorithms. In case 21a, compared with the original 119-bus system, the voltage deviation reduction obtained by the proposed algorithm has reached 95.79%, which is better than 95.72% by BF and 95.3% by PSO.

TABLE XI
CONFIGURATION INFORMATION OF DGS AND SCS IN 119-BUS SYSTEM FOR MINIMIZING *VD*

Methods	Location & size	case 17a (1 DGs, 1 SCs)	case 18a (2 DGs, 2 SCs)	case 19a (3 DGs, 3 SCs)	case 20a (4 DGs, 4 SCs)	case 21a (6 DGs, 6 SCs)
BF-CF	DG size KW (bus)	2949(111)	3915(81) 2983(111)	4034(38),4056(81) 3189(111)	4204(38),3262(68) 2729(81),3099(111)	3768(38),1749(50) 3079(68),2598(81) 1239(96),3030(111)
	SC size KVAR (bus)	2716(111)	3668(81) 2503(111)	2879(38),3998(81) 2515(111)	3003(38),2205(68) 2060(81),2505(111)	2801(38),1680(50) 1891(68),1960(81) 833(96),2577(111)
BF	DG size KW (bus)	3042(111)	4353(81) 2942(111)	3656(40),4169(81) 3015(111)	3506(40),3218(68) 2594(81),3093(111)	3417(40),1597(52) 3365(68),1487(85) 1710(98),3062(111)
	SC size KVAR (bus)	2589(111)	3363(81) 2496(111)	2512(40),3810(81) 2527(111)	2587(40),2061(68) 2081(81),2599(111)	2548(40),1633(52) 2013(73),1400(85) 1359(98),2570(111)
PSO	DG size KW (bus)	3084(111)	2830(82) 3010(111)	2948(42),2082(85) 3229(111)	3306(41),2773(73) 3443(80),3165(111)	3173(41),1485(53) 2667(73),3391(80) 1155(96),3143(111)
	SC size KVAR (bus)	2601(111)	2363(82) 2496(111)	3306(42),2474(85) 2300(111)	2713(41),2143(73) 2928(80),2617(111)	2552(41),1683(53) 1588(73),2823(80) 646(96),2470(111)

TABLE XII
RESULTS COMPARISON WITH BF AND PSO IN 119-BUS SYSTEM FOR MINIMIZING *VD*

Methods	parameters	base	case 17a	case 18a	case 19a	case 20a	case 21a
BF-CF	*VD* (p.u)	0.1875	**0.1515**	**0.0855**	**0.0402**	**0.0246**	**0.0079**
	P_T (KW)	978.10	739.92	615.65	458.24	285.04	158.23
	Q_T (KVAR)	718.80	585.44	462.61	276.07	192.72	105.30
	V_{max} (p.u)	1(1)	1.0039(111)	1.0198(81)	1.0233(81)	1.0106(38)	1.0084(81)
	V_{min} (p.u)	0.9293(113)	0.9305(89)	0.9326(44)	0.9475(53)	0.9477(53)	0.9738(27)
BF	*VD* (p.u)	0.1875	0.1516	0.0857	0.0411	0.0256	0.0080
	P_T (KW)	978.10	739.11	617.23	455.96	283.58	160.27
	Q_T (KVAR)	718.80	585.06	461.62	275.19	190.53	103.71
	V_{max} (p.u)	1(1)	1.0044(111)	1.0229(81)	1.0234(81)	1.0074(81)	1.0072(40)
	V_{min} (p.u)	0.9293(113)	0.9305(89)	0.9327(44)	0.9469(53)	0.9469(53)	0.9736(26)
PSO	*VD* (p.u)	0.1875	0.1516	0.0923	0.0509	0.0275	0.0088
	P_T (KW)	978.10	739.57	593.53	472.40	322.87	196.84
	Q_T (KVAR)	718.80	585.03	471.50	312.94	210.28	124.99
	V_{max} (p.u)	1(1)	1.0052(111)	1.0160(82)	1.0153 (42)	1.0156(80)	1.0158(80)
	V_{min} (p.u)	0.9293(113)	0.9305(89)	0.9327(44)	0.9469(53)	0.9469(53)	0.9735(27)

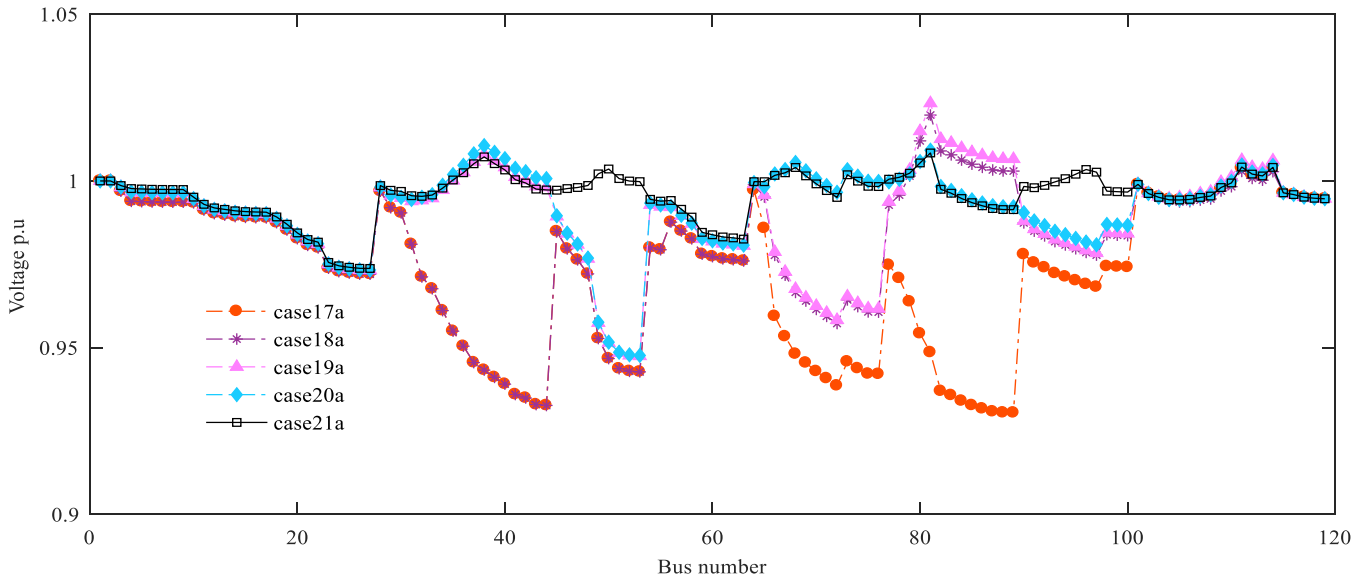

Fig. 28 Voltage profile for different case studies in 119-bus system for minimizing *VD* by BF-CF

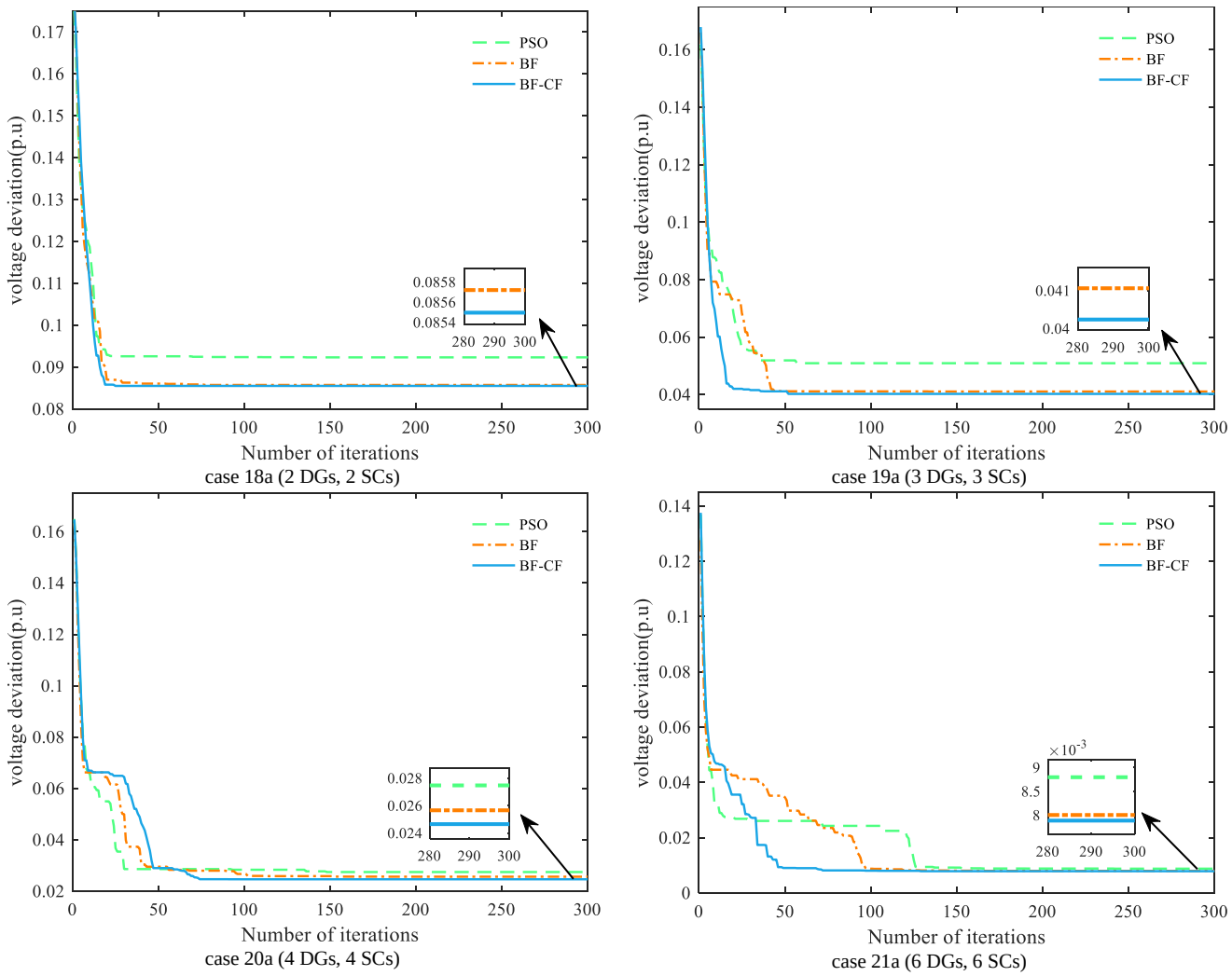

Fig. 29 Voltage deviation iteration curves in 119-bus system

The voltage deviation convergence characteristics shown in Fig. 29 further prove the superiority of the proposed algorithm in convergence speed and search accuracy. In case 21a, the voltage deviation converges to 0.0079 p.u after only 78 iterations by the BF-CF algorithm. Whereas the voltage deviation by the BF to converge to 0.0080 p.u needs 129 iterations, and the PSO requires 146 iterations to converge to 0.0088 p.u.

TABLE XIII compares the average and standard deviation of the voltage deviations of the three methods simulated 30 times. The mean and standard deviation of the voltage deviation obtained by BF-CF are superior to other methods, which indicates the proposed method is more suitable for the optimal configuration of DGs and SCs in complex systems.

TABLE XIII
THE AVERAGE VALUE AND STANDARD DEVIATION OF THE *VD* (p.u) IN 119-BUS SYSTEM

case	PSO		BF		BF-CF	
	mean	std	mean	std	mean	std
case 17a	0.1519	6.68E-06	0.1518	5.05E-06	0.1516	4.47E-06
case 18a	0.0924	0.000152	0.0884	0.000248	0.0856	0.000245
case 19a	0.0521	0.003847	0.0432	0.005194	0.0416	0.00412
case 20a	0.0277	9.58E-05	0.0281	0.005308	0.0255	0.002967
case 21a	0.0099	0.002523	0.0108	0.004619	0.0080	0.000177

The analysis of the above results figures that the method proposed in this paper can effectively solve the configuration problem of DGs and SCs in complex systems. Compared with the original BF and PSO algorithm, the BF-CF algorithm has evident advantages in improving system power loss and enhancing voltage stability.

V. CONCLUSION

This paper proposes a nodes processing method that combines the *PLI* and voltage amplitude of original systems and an improved butterfly algorithm with constriction factor to solve the problem of optimizing configuration of DGs and SCs in various RDNs, which simplifies the search space of the algorithm and achieves a balance between local search and global search. The objective function of minimizing active power loss and the reference index models of reactive power loss and voltage deviation are established. Under the premise of satisfying all constraints, multiple sets of simulation experiments are carried out on 33-bus, 69-bus, and 119-bus systems, and the effectiveness of the proposed method is verified. The results of active power loss, reactive power loss and voltage deviation obtained in this paper are compared with other intelligent algorithms, and comparisons with other methods indicate that the BF-CF algorithm has results with higher accuracy and faster convergence speed. In particular, when multiple DGs and multiple SCs are configured at the same time, the BF-CF algorithm can always obtain better active power loss, reactive power loss and voltage deviation values than other intelligent algorithms.

What's more, compared with the classic PSO and the original butterfly algorithm, BF-CF obtains results in a complex system with smaller power loss, higher accuracy and faster convergence speed, proving that BF-CF has powerful optimization search capabilities. Thus, the BF-CF algorithm combined with node processing is an effective method of solving the optimizing configuration of DGs and SCs in RDNs and improving system stability.

REFERENCES

[1] G. Chen, J. Qian, Z. Zhang, and Z. Sun, "Multi-objective improved bat algorithm for optimizing fuel cost, emission and active power loss in power system," *IAENG International Journal of Computer Science*, vol. 46, no. 1, pp. 118-133, 2019.

[2] G. Chen, S. Qiu, Z. Zhang, and Z. Sun, "Quasi-oppositional cuckoo search algorithm for multi-objective optimal power flow," *IAENG International Journal of Computer Science*, vol. 45, no. 2, pp. 255-266, 2018.

[3] X. Yuan, B. Ji, Z. Chen, and Z. Chen, "A novel approach for economic dispatch of hydrothermal system via gravitational search algorithm," *Applied Mathematics and Computation*, vol. 247, pp. 535-546, 2014.

[4] G. Chen, F. L. Lewis, E. N. Feng, and Y. Song, "Distributed optimal active power control of multiple generation systems," *IEEE Transactions on industrial Electronics*, vol. 62, no. 11, pp. 7079-7090, 2015.

[5] B. Poornazaryan, P. Karimyan, G. B. Gharehpetian, and M. Abedi, "Optimal allocation and sizing of DG units considering voltage stability, losses and load variations," *International Journal of Electrical Power & Energy Systems*, vol. 79, pp. 42-52, 2016.

[6] M. Yazdanian and A. Mehrizi-Sani, "Distributed control techniques in microgrids," *IEEE Transactions on Smart Grid*, vol. 5, no. 6, pp. 2901-2918, 2014.

[7] P. P. Biswas, R. Mallipeddi, P. N. Suganthan, and G. A. J. Amaratunga, "A multiobjective approach for optimal placement and sizing of distributed generators and capacitors in distribution network," *Applied Soft Computing*, vol. 60, pp. 268-280, 2017.

[8] A. Khodabakhshian and M. H. Andishgar, "Simultaneous placement and sizing of DGs and shunt capacitors in distribution systems by using IMDE algorithm," *International Journal of Electrical Power & Energy Systems*, vol. 82, pp. 599-607, 2016.

[9] A. A. El-Fergany, "Optimal capacitor allocations using evolutionary algorithms," *IET Generation Transmission & Distribution*, vol. 7, no. 6, pp. 593-601, 2013.

[10] R. S. Rao, S. V. L. Narasimham and M. Ramalingaraju, "Optimal capacitor placement in a radial distribution system using plant growth simulation algorithm," *International Journal of Electrical Power & Energy Systems*, vol. 33, no. 5, pp. 1133-1139, 2011.

[11] A. Zeinalzadeh, Y. Mohammadi and M. H. Moradi, "Optimal multi objective placement and sizing of multiple DGs and shunt capacitor banks simultaneously considering load uncertainty via MOPSO approach," *International Journal of Electrical Power & Energy Systems*, vol. 67, pp. 336-349, 2015.

[12] W. Sheng, K. Liu, Y. Liu, X. Meng, and Y. Li, "Optimal placement and sizing of distributed generation via an improved nondominated sorting genetic algorithm II," *IEEE Transactions on Power Delivery*, vol. 30, no. 2, pp. 569-578, 2015.

[13] A. K. Banhidarah and A. S. Al-Sumaiti, "Heuristic search algorithms for optimal locations and sizing of distributed generators in the grid: A brief recent review," *2018 Advances in Science and Engineering Technology International Conferences (ASET)*, Dubai, Sharjah, Abu Dhabi, United Arab Emirates, 2018.

[14] A. Selim, S. Kamel and F. Jurado, "Voltage stability analysis based on optimal placement of multiple DG types using hybrid optimization technique," *International Transactions on Electrical Energy Systems*, vol. 30, no. 10, article. e12551(1-20), 2020.

[15] S. Sharma, S. Bhattacharjee and A. Bhattacharya, "Quasi-oppositional swine influenza model based optimization with quarantine for optimal allocation of dg in radial distribution network," *International Journal of Electrical Power & Energy Systems*, vol. 74, pp. 348-373, 2016.

[16] M. Pesaran H. A, M. Nazari-Heris, B. Mohammadi-Ivatloo, and H. Seyedi, "A hybrid genetic particle swarm optimization for distributed generation allocation in power distribution networks," *Energy*, vol. 209, article. 118218(1-20), 2020.

[17] K. Balu and V. Mukherjee, "Siting and sizing of distributed generation and shunt capacitor banks in radial distribution system using constriction factor particle swarm optimization," *Electric Power Components and Systems*, vol. 48, no. 6-7, pp. 697-710, 2020.

[18] M. Jegadeesan, C. K. Babulal and V. Subathra, "Simultaneous placement of multi-DG and capacitor in distribution system using hybrid optimization method," *2017 International Conference on Innovations in Green Energy and Healthcare Technologies (IGEHT)*, Coimbatore, India, 2017.

[19] K. Muthukumar and S. Jayalalitha, "Integrated approach of network reconfiguration with distributed generation and shunt capacitors placement for power loss minimization in radial distribution networks," *Applied Soft Computing*, vol. 52, pp. 1262-1284, 2017.

[20] K. Muthukumar and S. Jayalalitha, "Optimal placement and sizing of distributed generators and shunt capacitors for power loss minimization in radial distribution networks using hybrid heuristic search optimization technique," *International Journal of Electrical Power & Energy Systems*, vol. 78, pp. 299-319, 2016.

[21] M. H. Moradi, A. Zeinalzadeh, Y. Mohammadi, and M. Abedini, "An efficient hybrid method for solving the optimal sitting and sizing problem of DG and shunt capacitor banks simultaneously based on imperialist competitive algorithm and genetic algorithm," *International Journal of Electrical Power & Energy Systems*, vol. 54, pp. 101-111, 2014.

[22] M. Mohammadi, A. M. Rozbahani and S. Bahmanyar, "Power loss reduction of distribution systems using BFO based optimal reconfiguration along with DG and shunt capacitor placement simultaneously in fuzzy framework," *Journal of Central South University*, vol. 24, no. 1, pp. 90-103, 2017.

[23] A. K. Bohre, G. Agnihotri and M. Dubey, "The butterfly-particle swarm optimization (Butterfly-PSO/BF-PSO) technique and its variables," *International Journal of Soft Computing, Mathematics and Control*, vol. 4, no. 3, pp. 23-39, 2015.

[24] M. M. Aman, G. B. Jasmon, A. H. A. Bakar, and H. Mokhlis, "Optimum network reconfiguration based on maximization of system loadability using continuation power flow theorem," *International Journal of Electrical Power & Energy Systems*, vol. 54, pp. 123-133, 2014.

[25] A. El-Fergany, "Optimal allocation of multi-type distributed generators using backtracking search optimization algorithm," *International Journal of Electrical Power & Energy Systems*, vol. 64, pp. 1197-1205, 2015.

[26] M. M. Aman, G. B. Jasmon, K. H. Solangi, A. H. A. Bakar, and H. Mokhlis, "Optimum simultaneous DG and Capacitor placement on the basis of minimization of power losses," *International Journal of Computer and Electrical Engineering*, vol. 5, no. 5, pp. 516-522, 2013.

[27] K. Gholami and M. H. Parvaneh, "A mutated salp swarm algorithm for optimum allocation of active and reactive power sources in radial distribution systems," *Applied Soft Computing*, vol. 85, article. 105833(1-41), 2019.

[28] A. Khodabakhshian and M. H. Andishgar, "Simultaneous placement and sizing of DGs and shunt capacitors in distribution systems by using IMDE algorithm," *International Journal of Electrical Power & Energy Systems*, vol. 82, pp. 599-607, 2016.

[29] E. A. Almabsout, R. A. El-Sehiemy, O. N. U. An, and O. Bayat, "A hybrid local search-genetic algorithm for simultaneous placement of DG units and shunt capacitors in radial distribution systems," *IEEE Access*, vol. 8, pp. 54465-54481, 2020.

[30] A. Youssef, S. Kamel, M. Ebeed, and J. Yu, "Optimal capacitor allocation in radial distribution networks using a combined optimization approach," *Electric Power Components and Systems*, vol. 46, no. 19-20, pp. 2084-2102, 2018.

[31] K. H. Truong, P. Nallagownden, I. Elamvazuthi, and D. N. Vo, "A quasi-oppositional-chaotic symbiotic organisms search algorithm for optimal allocation of DG in radial distribution networks," *Applied Soft Computing*, vol. 88, article. 106067(1-53), 2020.

[32] N. Kanwar, N. Gupta, K. R. Niazi, and A. Swarnkar, "Improved meta-heuristic techniques for simultaneous capacitor and DG allocation in radial distribution networks," *International Journal of Electrical Power & Energy Systems*, vol. 73, pp. 653-664, 2015.